Microwave Spectra of the Free Radicals OH and OD*

G. C. DOUSMANIS, T. M. SANDERS, JR.,† AND C. H. TOWNES
Physics Department, Columbia University, New York, New York

(Received August 18, 1955)

Experiments are reported on the microwave spectra of the free OH radical. The radicals are produced by an electric discharge in concentrations near 10% at pressures of approximately 0.1 mm Hg. The spectra are detected by Zeeman modulation. They are due to direct transitions between the Λ-doublet levels of each rotational state in the ground vibrational level of the molecule. Spectra due to $O^{16}H$, $O^{18}H$, and $O^{16}D$ in $^2\Pi_{\frac{3}{2}}$ and $^2\Pi_{\frac{1}{2}}$ states have been observed in the 7.7 to 37 kMc/sec region. Intensity of the lines ranges from about 5×10^{-6} cm^{-1} to 5×10^{-8} cm^{-1}.

Van Vleck's theory of molecular energies in $^2\Pi$ and $^2\Sigma$ states is extended to include terms of order $(E_{\text{rot}}$ or $E_{fs})^2/E_{\text{el}}^2$. The experimental results are in agreement with theoretical expectations to about one part in 2000 which is the order of accuracy of the theory. An improved agreement (to one part in 3500) is obtained if one allows a small variation (one part in 1400) of the electronic wave function from one rotational state to the next. The values of the molecular constants determined from the Λ-type doubling data are

$$4\sum_{\Sigma\text{-states}}(-1)^s\langle\Pi|AL_y+2BL_y|\Sigma\rangle\langle\Sigma|BL_y|\Pi\rangle/(E_\Sigma-E_\Pi)$$
$$=-2361.37\pm2.95 \text{ Mc/sec in } O^{16}H$$
and -1548.99 ± 2.10 Mc/sec in $O^{16}D$;

$$4\sum_{\Sigma\text{-states}}(-1)^s|\langle\Pi|BL_y|\Sigma\rangle|^2/(E_\Sigma-E_\Pi)=576.18\pm1.64 \text{ Mc/sec}$$
in $O^{16}H$ and 161.94 ± 1.61 Mc/sec in $O^{16}D$;

$A/B=-7.444\pm0.017$ in $O^{16}H$ and -13.954 ± 0.032 in $O^{16}D$. The spectra include magnetic hyperfine structure from which the following values are obtained for parameters that describe the unpaired electron distribution in the molecule:

$$(1/r^3)_{Av}=(0.75\pm0.25)\times10^{24} \text{ cm}^{-3}$$

and

$$(\sin^2\chi/r^3)_{Av}=(0.49\pm0.01)\times10^{24} \text{ cm}^{-3}.$$

The hyperfine structure, the molecular magnetic moment and the line intensities are strongly dependent on the extent of intermediate coupling in agreement with theoretical expectations. The microwave spectrum can be used in studying chemical properties of the radical. Its lifetime was determined to be near $\frac{1}{3}$ sec, and the effects of certain substances on radical concentration were examined.

1. INTRODUCTION

FREE radicals are unstable molecules or molecular fragments which usually possess one or more unpaired electrons. They are chemically very reactive substances with short lifetimes in most cases much less than one second. Many have been detected, or postulated to be present, in electrical discharges, flames, detonations, and in the gas of comets.

The ground electronic state of many free radicals, in contrast to the vast majority of stable molecules, is not a $^1\Sigma$ state. In addition to the rotational terms, their energy levels show prominent fine structure and effects of coupling between rotation and electronic motion such as Λ-type doubling, p-type doubling etc.

Study of free radicals by microwave spectroscopy should yield detailed information on their energy level structure and, in addition, one might use the microwave spectrum to obtain information on their lifetimes, and the kinetics of chemical processes.

Unstable molecules have been produced in a variety of ways, e.g., by electric discharges, photolysis, and pyrolysis. In the experiments to be described, electric discharges were used, largely because this seemed the simplest method for our purposes.

Since the plasma of an electric discharge will attenuate microwaves strongly, the radicals must be examined either in a different location or at a different time from that at which they are produced. In either case the radicals must, of course, not be permitted to recombine before they are observed. The choice of materials for the surfaces with which radicals come in contact, in view of their high degree of reactivity, is of paramount importance. In addition, charged particles produced in the discharge should not be present to any large extent when the gas is examined by microwaves. In the present experiments, the discharge tube and the absorption cell were separated in space, the radicals flowing into the absorption cell through a glass tube. The alternative method of examining the radicals in the place they are produced but at a slightly later time could be particularly useful in the study of very short-lived substances. This advantage however would probably be accompanied by considerable complication of the apparatus.

For the detection of the spectra a rather conventional modulation spectrometer[1] with associated narrow-band amplifier and phase sensitive detector was constructed. However, advantage was taken of the large magnetic moment exhibited by many free radicals. Modulation was accomplished by radio-frequency variation of a magnetic field rather than the usual electric field. Such a modulation scheme simplifies the searching problem since the spectra of stable molecules, which may be used as the source of radicals, are not detectable with the Zeeman spectrometer. The method also makes it unnecessary to obstruct the wave guide with a metal

* Work supported jointly by the Department of the Army (Signal Corps), the Department of the Navy (Office of Naval Research), and the Department of the Air Force (Air Research and Development Command).

† RCA Fellow, now at Physics Department, University of Minnesota, Minneapolis, Minnesota.

[1] A. H. Sharbaugh, Rev. Sci. Instr. **21**, 120 (1950).

septum which would reduce the pumping speed and produce a disastrous amount of recombination of radicals.

Precise information on free radicals, obtained from optical or near-optical spectroscopic work, is very scarce. One is therefore confronted with a searching problem, since in most cases the microwave spectra cannot be predicted with much accuracy. Although the situation is much worse than in the case of stable molecules, this searching problem is certainly not as formidable as the ones connected with their instability.

The OH radical was selected for study because it had been the subject of a considerable amount of quantitative work. The lifetime of the radical was known to be relatively long[2] and the absorption frequencies to be expected[3] in the microwave region, could be predicted with sufficient accuracy to render the search problem not too prohibitive. It was further believed possible to establish the presence of the radicals by other than spectroscopic means.[4,5] This last would provide a check on the operation of the production and transport phase of the experiment.

The ground electronic state of OH is a $^2\Pi$. The particular lines that have been observed in this work are due to transitions between the two members of the Λ-type doublet into which each J level is split. Spectra have been observed in both the $\Pi_{\frac{3}{2}}$ and $\Pi_{\frac{1}{2}}$ states of the ground vibrational level. The OH radical is so light that its rotational spectrum lies in the far infrared. It is only because the electronic angular momenta are not zero that transitions appear in the microwave region.

2. EXPERIMENTAL TECHNIQUES

(a) Production of OH–Vacuum System

The OH is produced by a discharge through water vapor. The all-glass vacuum system (Fig. 1) consists of a water source, a discharge tube of 28 mm Pyrex, the absorption cell, a pair of connecting tubes of 18 mm Pyrex and a liquid nitrogen trap located near the output end of the absorption cell. The cell itself consists of a Corning 707 glass tube, 150 cm long and 30 mm in diameter. Type 707 glass was used because of its low dielectric loss at microwave frequencies. In the early part of this work[6] a much shorter (75 cm) absorption cell was in use. The glass tube in the absorption cell is sealed at both ends and these ends are blown to minimum thickness (to facilitate microwave transmission) consistent with adequate strength. The system is pumped by a Welch type 1397B mechanical pump and, if needed, a DPI MB-100 oil diffusion pump. In the experiments described here use of the diffusion pump was not necessary.

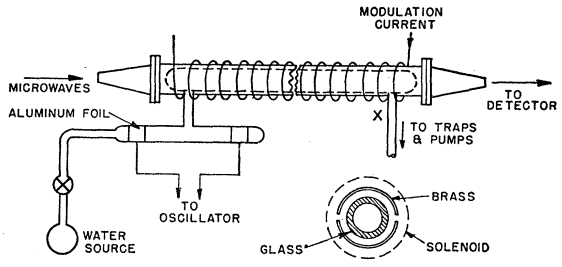

FIG. 1. Vacuum system and absorption cell.

Under the operating conditions of continuous flow about 3 g of water leave the source per hour. The water vapor enters the discharge tube and the discharge products flow into the absorption cell and from there to the liquid nitrogen trap and pumps. A thermocouple gauge located at point X (Fig. 1) indicates a pressure near 0.1 mm Hg. This figure must be taken with some reservations since (1) recombination of radicals occurs on the thermocouple wires, giving rise to spurious temperature readings; (2) the gauge reading is dependent on the composition of the gas which is not known and which varies with discharge conditions.

The discharge is maintained either with a dc supply and aluminum electrodes, or as shown in Fig. 1, with external aluminum foil electrodes and power supplied by a 300-watt oscillator operating in the vicinity of two megacycles. The high-pressure limit on the stable operation of the discharge is set by its tendency, at high pressures, to pass from one electrode into the absorption cell rather than between the two electrodes. This tendency of the discharge to "jump" inside the absorption cell can be appreciably reduced by a horseshoe magnet placed around the glass tube connecting the discharge tube with the absorption cell.

The abundance of radicals in the absorption cell, as measured by the intensity of the microwave lines, is strongly dependent on pressure and discharge current.[7] In the present apparatus it is not simple to distinguish between changes in the rate of production of the radicals and in the rate of their subsequent disappearance through recombination. It may be noted that maximum intensity is produced with only moderate excitation. Under conditions of optimum line intensity, the dc power input to the oscillator is in the neighborhood of 100 watts. To obtain comparable radical abundance with the dc discharge, more than 500 watts must be supplied. The discharge is normally powered by the two-megacycle oscillator.

[2] O. Oldenberg, J. Chem. Phys. **3**, 266 (1935).
[3] G. H. Dicke and R. M. Crosswhite, Bumblebee Report No. 87, Johns Hopkins University, November, 1948 (unpublished); Hicks, Ossofsky and Jones, Technical Note No. 130, Ballistic Research Laboratories, Aberdeen Proving Ground, Maryland, November, 1949 (unpublished).
[4] W. H. Rodebush and M. H. Wahl, J. Chem. Phys. **1**, 696 (1933); R. W. Campbell and W. H. Rodebush, J. Chem. Phys. **4**, 293 (1936).
[5] H. S. Taylor and G. I. Lavin, J. Am. Chem. Soc. **52**, 1910 (1930). W. V. Smith, J. Chem. Phys. **11**, 110 (1943).
[6] Sanders, Schawlow, Dousmanis, and Townes, Phys. Rev. **89**, 1158 (1953); G. C. Dousmanis, Phys. Rev. **94**, 789 (A) (1954).
[7] Sanders, Schawlow, Dousmanis, and Townes, J. Chem. Phys. **22**, 245 (1954).

(b) Microwave Spectrometer

We confine the description of the microwave spectrometer to the wave guide enclosing the absorption cell and the apparatus for Zeeman modulation. The other components and detection circuits are those of a conventional Stark modulation spectrometer[1] and need not be described here.

A brass pipe, split in half (Fig. 1) and with holes for input and output tubes is mounted around the glass tubing. It operates as a cylindrical wave guide in the dominant (TE_{11}) mode. Microwave power enters and leaves the absorption cell through tapered sections which establish connection with standard sizes of rectangular wave guide. The microwave properties of this system are inferior to those of a Stark modulation cell. The presence of the glass cell inside the wave-guide results in an attenuation of the transmitted power by a factor of about 30. In addition, as the microwave frequency is varied the transmission varies as a result of reflections due to the glass, the tapered sections and the large holes cut in the wave guide. Despite these shortcomings sufficient power can be transmitted through the system for spectroscopic work in the region from 7000 to about 45 000 Mc/sec.

Magnetic fields of a few gauss are produced by a close-wound single layer coil of No. 14 wire wound over the wave guide. Since this magnetic field is axial, and the wave guide is operated in a TE mode only $\Delta M=\pm 1$ Zeeman components of electric dipole transitions are observed. During the greater part of these experiments a modulation frequency near 227 kc/sec was used. Modulation at a frequency of 100 kc/sec, which was used in the earlier part of this work,[6] is equally effective.

The best sensitivity with such a system may be obtained by use of a square current wave form. However, production of this type of wave in the coil (whose self-resonance frequency is approximately one megacycle) appeared so formidable a problem that a sine wave plus an appropriate amount of dc bias were used instead.

The sentivity of the instrument was determined by comparison with a Stark spectrometer of known sensitivity. Microwave absorption lines of NO_2 and ClO_2 were examined with both instruments, and the sensitivity (minimum detectable absorption) was found to be near 10^{-8} cm^{-1}. A somewhat low sensitivity is to be expected, because of the inefficient modulation system.

(c) Intensity Considerations

The intensity to be expected for one Λ-type doubling transition in OH could not be calculated accurately before any measurements were made, because of several uncertainties. First, the abundance of radicals which may be expected to be present in the absorption cell was not known. Second, the permanent electric dipole moment of OH is unknown. Third, one could not predict with precision the width of the OH lines at any particular pressure.

An expression for the peak absorption coefficient of a microwave line is[8,9]

$$\gamma_{\max}=\frac{8\pi^2 Nf|\mu_{ij}|^2\nu^2}{3ckT\Delta\nu}, \tag{1}$$

where Nf is the number of molecules per cm^3 in the lower state of transition, $|\mu_{ij}|^2$=square of matrix element of the dipole moment (electric in our case) for the transition, ν=frequency of transition, and $\Delta\nu$=half-width of the line at one half maximum intensity.

Assuming thermal equilibrium, the fraction of OH molecules in any state may be evaluated, since the energy level structure is well known. The form of the dipole moment matrix element is well known[9] in the approximation of pure Hund's case (b) coupling:

$$|\mu_{ij}|^2=\mu^2\Lambda^2/(J+1)(2J+1). \tag{2}$$

[The effect of intermediate coupling on the matrix element will be discussed in Sec. 4(f).]

Inserting numerical values in (1) for the $J=9/2$ Λ-type doubling transition in the $^2\Pi_{\frac{3}{2}}$ state of OH at $\nu\sim$23 800 Mc/sec, one obtains for a single hyperfine component

$$\gamma_{\max}=2\times10^{-6}(\beta\mu^2/\Delta\nu)\text{ cm}^{-1},$$

where β is the percentage of all molecules which are OH radicals. μ is the dipole moment in Debye units and $\Delta\nu$ the line breadth parameter in (Mc/sec) per mm. Inserting the tentative values[10] $\mu=1.5$ and $\Delta\nu=5$, we obtain

$$\gamma_{\max}=0.9\beta\times10^{-6}\text{ cm}^{-1}.$$

Two previous determinations of the abundance of OH radicals were available. The first, obtained from measurements on the ultraviolet spectrum of OH produced by thermal dissociation of water, and in dc discharges yields an abundance in the latter case[11–13] of about 0.1%. With abundance of this order we would have in the present work $\gamma_{\max}\sim9\times10^{-8}$ cm^{-1}, which is detectable, but with some difficulty.

The second method is less direct, and consists in inferring the radical abundance in the vapor from the concentration of H_2O_2 in the condensate produced on the liquid nitrogen trap exposed to this vapor.[4] This method rests on a belief that the mechanism responsible for the production of H_2O_2 is $OH+OH+M\rightarrow H_2O_2$,[14]

---

[8] J. H. Van Vleck and V. Weisskoff, Revs. Modern Phys. **17**, 228 (1945).

[9] C. H. Townes and A. L. Schawlow, *Microwave Spectroscopy* (McGraw-Hill Book Company, Inc., New York, 1955).

[10] R. P. Madden and W. S. Benedict, J. Chem. Phys. **23**, 408 (1955).

[11] A. A. Frost and O. Oldenberg, J. Chem. Phys. **4**, 642 (1936).

[12] O. Oldenberg and F. F. Rieke, J. Chem. Phys. **6**, 439 (1938); **7**, 485 (1939).

[13] R. J. Dwyer and O. Oldenberg, J. Chem. Phys. **12**, 351 (1944).

[14] See K. H. Geib, J. Chem. Phys. **4**, 391 (1938) for objections to such a mechanism of H_2O_2 production.

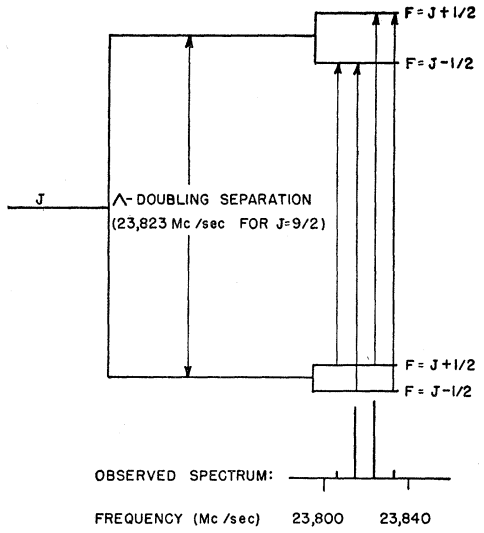

FIG. 2. Diagram indicating the Λ-type doubling and hyperfine structure in one rotational level of the $\Pi_{\frac{3}{2}}$ state of $O^{16}H$. The spectrum shown is that of the $J=9/2$ level.

where M is a third body in or on the trap walls. H_2O_2 concentrations as high as 50% have been obtained both by the original experimenters and the present workers, leading to the conclusion that the dissociation of H_2O is nearly complete. From the above expression, $\beta=50\%$ gives $\gamma_{max}=4.5\times10^{-5}$ cm^{-1}, or a signal-to-noise ratio of about 4000 or more. However, these tests for OH were found to need re-evaluation when the microwave spectrum was detected.

3. OBSERVED SPECTRA OF OH AND OD

Each rotational level of OH, in both the $\Pi_{\frac{1}{2}}$ and the $\Pi_{\frac{3}{2}}$ states, is split into a Λ-type doublet. Each component of the doublet is further split by magnetic hyperfine structure, due to hydrogen or deuterium, into components characterized by the total angular momentum $\mathbf{F}(=\mathbf{J}+\mathbf{I})$. F, of course, takes on the values $J+\frac{1}{2}$ and $J-\frac{1}{2}$ in OH, and $J+1$, J and $J-1$ in OD. Figure 2 shows the energy level arrangement for $J=9/2$ in the $\Pi_{\frac{3}{2}}$ state of OH.

From the selection rule $\Delta F=0, \pm1$, every Λ-type doubling transition is expected to be split into four hyperfine components in OH and seven in OD. In transitions of the type $\Delta J=0$, the hyperfine lines arising from the $\Delta F=0$ transitions will be the strongest. There are two such components in OH and three in OD. The $\Delta F=\pm1$ transitions ("satellite" lines) are much weaker[15] than the main ($\Delta F=0$) lines. These satellites have been observed in the strongest of the Λ-doubling transitions ($J=9/2$ $\Pi_{\frac{3}{2}}$ state) in OH that are reported here.

Transitions due to several rotational states of $O^{16}H$, $O^{18}H$, and $O^{16}D$, in both the $\Pi_{\frac{1}{2}}$ and $\Pi_{\frac{3}{2}}$ states have been observed. The observed signal to noise ratio ranges from 10/1 ($\Pi_{\frac{1}{2}}$ state, $J=11/2$ of OD) to about 1000/1 ($\Pi_{\frac{3}{2}}$ state, $J=9/2$ of OH). The $O^{18}H$ spectrum was obtained with a water sample enriched to 1.4% in O^{18}. A representative value of the line half-width at one-half maximum intensity is about 800 kc/sec. This rather large width is due to a somewhat higher (0.1 mm Hg) pressure than is usual for microwave spectroscopy and to the sine wave modulation.

The measured frequencies and their quantum assignments are given in Table I. The quantum number N designates the sum of the electron orbital ($\mathbf{\Lambda}$) and the rotational angular momentum. $\mathbf{J}$ is $\mathbf{N}+\mathbf{S}$ and equals $N+\frac{1}{2}$ in the $\Pi_{\frac{3}{2}}$ state and $N-\frac{1}{2}$ in the $\Pi_{\frac{1}{2}}$ state. It is

TABLE I. Frequencies of the observed Λ-type doubling transitions in OH and OD.

Molecule	Electronic state	N	J	Hyperfine transition	Experimental frequency (Mc/sec)
$O^{16}H$	$\Pi_{\frac{1}{2}}$	2	3/2	$F=1\rightarrow F=1$	7 760.36±0.15
				$F=2\rightarrow F=2$	7 819.92±0.10
		3	5/2	$F=2\rightarrow F=2$	8 135.51±0.15
				$F=3\rightarrow F=3$	8 188.94±0.10
	$\Pi_{\frac{3}{2}}$	3	7/2	$F=3\rightarrow F=3$	13 434.62±0.05
				$F=4\rightarrow F=4$	13 441.36±0.05
		4	9/2	$F=5\rightarrow F=4$	23 806.5 ±0.5
				$F=4\rightarrow F=4$	23 818.18±0.05
				$F=5\rightarrow F=5$	23 826.90±0.05
				$F=4\rightarrow F=5$	23 837.8 ±0.3
		5	11/2	$F=5\rightarrow F=5$	36 983.47±0.15
				$F=6\rightarrow F=6$	36 994.43±0.15
$O^{18}H$	$\Pi_{\frac{3}{2}}$	4	9/2	$F=4\rightarrow F=4$	23 469.5 ±0.5
				$F=5\rightarrow F=5$	23 479.1 ±0.5
$O^{16}D$	$\Pi_{\frac{1}{2}}$	3	5/2	$F=3/2\rightarrow F=3/2$	8 110.20±0.10
				$F=5/2\rightarrow F=5/2$	8 117.69±0.10
				$F=7/2\rightarrow F=7/2$	8 127.64±0.15
		4	7/2	$F=5/2\rightarrow F=5/2$	9 578.51±0.15
				$F=7/2\rightarrow F=7/2$	9 586.03±0.10
				$F=9/2\rightarrow F=9/2$	9 595.26±0.10
		5	9/2	$F=7/2\rightarrow F=7/2$	10 191.64±0.10
				$F=9/2\rightarrow F=9/2$	10 199.10±0.10
				$F=11/2\rightarrow F=11/2$	10 208.14±0.10
		6	11/2	$F=9/2\rightarrow F=9/2$	9 914.39±0.10
				$F=11/2\rightarrow F=11/2$	9 921.53±0.10
				$F=13/2\rightarrow F=13/2$	9 929.88±0.10
$O^{16}D$	$\Pi_{\frac{3}{2}}$	5	11/2	$F=9/2\rightarrow F=9/2$, $F=11/2\rightarrow F=11/2$, $F=13/2\rightarrow F=13/2$	8 672.36±0.10
		6	13/2	$F=11/2\rightarrow F=11/2$, $F=13/2\rightarrow F=13/2$, $F=15/2\rightarrow F=15/2$	12 918.01±0.10
		7	15/2	$F=13/2\rightarrow F=13/2$, $F=15/2\rightarrow F=15/2$, $F=17/2\rightarrow F=17/2$	18 009.60±0.10
		8	17/2	$F=15/2\rightarrow F=15/2$, $F=17/2\rightarrow F=17/2$, $F=19/2\rightarrow F=19/2$	23 907.12±0.10

[15] Relative intensities for the hyperfine components are given in reference 9 and elsewhere.

noted that the quantum number N is well defined only for the higher rotational states.

The initial assignment[6] N,J for the $^2\Pi_{\frac{3}{2}}$ state of OH was based on ultraviolet data.[3] However, these quantum numbers can be assigned from the fact that the frequencies of any two of the observed transitions of OD or of the $^2\Pi_{\frac{1}{2}}$ state of OH allow, with the proper assignment, accurate prediction of all the other frequencies. The assignment is furthermore confirmed by relative intensity measurements and the observed hfs patterns.

Assignment of the quantum number F is based on the observed relative intensities of the strongest ($\Delta F=0$) hyperfine components for a given J, which should be approximately proportional to the respective values of F.

One might be surprised that transitions due to the $^2\Pi_{\frac{1}{2}}$ state have been detected with a magnetic spectrometer. The magnetic moment in this state, in a pure Hund's case (a) quantization would be expected to be close to zero as a result of cancellation of the contributions from the electron orbital motion and the electron spin. However, the rotational energy will gradually decouple the spin from the orbital angular momentum [intermediate coupling between Hund's cases (a) and (b)]. This spin uncoupling effect introduces a substantial magnetic moment into the $^2\Pi_{\frac{1}{2}}$ state even for as low a value of J as $\frac{3}{2}$, and makes possible the Zeeman modulation of the spectra by magnetic fields of about 5 gauss. A more detailed discussion of the molecular magnetic moment appears in Sec. 4(d).

4. THEORY

(a) The Hamiltonian, Wave Functions in the Intermediate Coupling State, and Approximate Energies

The molecular Hamiltonian involves (a) the rotational terms and the fine structure interaction $\mathbf{L}\cdot\mathbf{S}$ (designated hereafter as H_1), (b) magnetic hyperfine structure (H_2), and (c) the interaction with an external magnetic field (H_3). The interaction due to the quadrupole moment of the deuteron is expected to be small and will not be discussed since the observed hyperfine structure in OD can be accounted for within the present experimental error by the magnetic hyperfine interaction alone.

H_{total} is then taken as $H_1+H_2+H_3$, where

$$\begin{aligned}H_1&=B[(J_x-S_x-L_x)^2+(J_y-S_y-L_y)^2]\\&\quad+AL_zS_z+A(L_xS_x+L_yS_y)\\&=B[J(J+1)-\Lambda^2]+BS(S+1)+AL_zS_z-2B\mathbf{J}\cdot\mathbf{S}\\&\quad+B(L_x^2+L_y^2)+(2B+A)(L_xS_x+L_yS_y)\\&\quad-2B(J_xL_x+J_yL_y).\end{aligned}\tag{3}$$

The z direction is along the internuclear axis. As usual, A and B designate the fine structure interaction and rotational constants respectively, $\mathbf{L}$ and $\mathbf{S}$ the electron orbital and spin angular momenta, and $\mathbf{J}$ the total molecular angular momentum exclusive of nuclear spin. Λ is the quantum number associated with L_z. Definitions of the various symbols used and values of the constants in OH and OD are given in Appendix I.

The first two lines in (3) give rise to the rotational and spin-orbit interaction energies; these terms are diagonal in Λ. The term $B(L_x^2+L_y^2)$ is diagonal in Λ and, to a high order of approximation, independent of J. Hence it adds to the energy a constant that will be ignored for the moment. The terms $(2B+A)(L_xS_x+L_yS_y)$ and $-2B(J_xL_x+J_yL_y)$ are off-diagonal in Λ and give rise to the Λ-type doubling. Note that A and B are the fine structure and rotational constants with their usual meaning only in those terms of (3) that are diagonal in Λ.

The magnetic hyperfine and Zeeman parts of the Hamiltonian (H_2 and H_3) are discussed in Secs. 4(c) and 4(d), respectively. In the present section the eigenvalues arising from H_1 will be given and wave functions constructed for $^2\Pi$ states in the general coupling scheme, intermediate between Hund's cases (a) and (b). These wave functions are necessary for the calculation of the molecular magnetic moment, the hyperfine structure and the electric dipole moment matrix element, since the experimental data indicate a strong dependence of these quantities on the extent of intermediate coupling.

The matrix elements of H_1 have been given by Van Vleck[16] on the basis of wave functions that correspond to a Hund's case (a) coupling scheme. In this representation both the electron orbital and spin angular momenta are quantized along the internuclear axis with eigenvalues Λ and Σ, respectively. The total angular momentum along the axis is designated by $\Omega(=\Lambda+\Sigma)$. The angular momentum due to the end over end rotation of the nuclei is added to Ω to form J.

There are six states to be considered: $\Pi_{\frac{3}{2}}$, $\Pi_{-\frac{3}{2}}$, $\Pi_{\frac{1}{2}}$, $\Pi_{-\frac{1}{2}}$, $\Sigma_{\frac{1}{2}}$, $\Sigma_{-\frac{1}{2}}$. The interactions between all pairs of states form a six-by-six determinant which can be factored[16] into two cubics by introducing wave functions of the symmetric and antisymmetric type rather than those that represent angular momentum of constant sign about the internuclear axis. In terms of the previous set ($\Pi_{\frac{3}{2}}$, $\Pi_{-\frac{3}{2}}$, etc.) the new wave functions are

$$\psi_{\text{sym, ant.}}=[\psi(\Lambda,\Sigma,\Omega)\pm\psi(-\Lambda,-\Sigma,-\Omega)]/\sqrt{2}.\tag{4}$$

One of the two 3-by-3 determinants into which the secular equation factors is

$$\begin{array}{c|ccc|}&\Sigma_{\frac{1}{2}}&\Pi_{\frac{1}{2}}&\Pi_{\frac{3}{2}}\\ \Sigma_{\frac{1}{2}}&\kappa-\lambda&\mu&\eta\\ \Pi_{\frac{1}{2}}&\mu^*&\beta-\lambda&\epsilon\\ \Pi_{\frac{3}{2}}&\eta^*&\epsilon^*&\gamma-\lambda\end{array}.\tag{5}$$

The matrix elements, as given by Van Vleck,[16] along with the phase conventions to be observed, are reproduced in Appendix II. In (5), $\kappa=\alpha+\delta$ and $\mu=\theta+\zeta$,

[16] J. H. Van Vleck, Phys. Rev. **33**, 467 (1929).

where

$$\alpha\equiv E_\Sigma-E_\Pi+B_s(J+\tfrac{1}{2})^2,\quad \delta\equiv(-1)^s B_s(J+\tfrac{1}{2}),$$
$$\theta\equiv\langle\Pi|AL_y+2BL_y|\Sigma\rangle$$

and

$$\zeta\equiv(-1)^s 2\langle\Pi|BL_y|\Sigma\rangle(J+\tfrac{1}{2}).$$

The other cubic determinant is identical with (5) except that $\kappa=\alpha-\delta$ and $\mu=\theta-\zeta$.

Our procedure in this paper is to diagonalize (5) to successively higher orders of approximation. The energies can be written (order of magnitude) as

$$E\sim[(1+A/B+(B\text{ or }A)/E_{\text{elec}}+((B\text{ or }A)/E_{\text{elec}}))^2+\cdots]B. \quad (6)$$

The expansion parameters, then are $(E_{\text{rotational}}/E_{\text{electronic}})$, and $(E_{\text{fine structure}}/E_{\text{electronic}})$.[17] $E_{\text{elec}}=E_\Sigma-E_\Pi$. With the constants[18] $A=-139.7$ cm^{-1}, $B=18.52$ cm^{-1}, and $E=32\,682.5$ cm^{-1}, the numerical values of the expansion parameters in OH are $(B/E)=1/1765$ and $(A/E)=1/234$. (In other molecules the values are of the same general order of magnitude and in all cases the expansion converges rather rapidly.) A representative figure for our experimental accuracy is one part in 150 000. Hence the expansion should include terms of at least second order in the expansion parameters. Even the third order term $[(B\text{ or }A)^3/E_{\text{el}}{}^3]B$ is actually somewhat larger than the experimental error. There are, however, several other small effects of the same order of magnitude (see Sec. 5a) that are neglected; hence inclusion of this term alone would not be justified. The terms of (6) will be corrected, to the appropriate order, for effects of coupling of rotation to vibrational motion, i.e., B is to be taken as $B_v[=B_e-(v+\frac{1}{2})\alpha_e]$, where α_e is the vibration-rotation interaction constant and also is to be corrected for centrifugal distortion.

The two Π states are only 140 cm^{-1} apart, whereas the Σ state lies 32 683 cm^{-1} above them. Hence the rotational and spin-orbit energies [zero-order term in (6)] can be obtained by diagonalizing the submatrix

$$\begin{pmatrix}\beta-\lambda & \epsilon\\ \epsilon^* & \gamma-\lambda\end{pmatrix}. \quad (7)$$

The result is[16]

$$\lambda=\tfrac{1}{2}(\beta+\gamma)\pm\tfrac{1}{2}[(\beta-\gamma)^2+4|\epsilon|^2]^{\frac{1}{2}}=\tfrac{1}{2}(\beta+\gamma)\pm\tfrac{1}{2}B_pX, \quad (8)$$

where

$$X\equiv+[4(J+\tfrac{1}{2})^2+\lambda(\lambda-4)]^{\frac{1}{2}},\quad \lambda\equiv A/B_p. \quad (9)$$

The diagonalization of (7) yields in addition the needed wave functions:

$$\psi_{\text{Int. }1}=\left(\frac{X-2+\lambda}{2X}\right)^{\frac{1}{2}}\psi(\Pi_{\frac{1}{2}})\mp\left(\frac{X+2-\lambda}{2X}\right)^{\frac{1}{2}}\psi(\Pi_{\frac{3}{2}}),$$
$$\psi_{\text{Int. }2}=\pm\left(\frac{X-2+\lambda}{2X}\right)^{\frac{1}{2}}\psi(\Pi_{\frac{3}{2}})+\left(\frac{X+2-\lambda}{2X}\right)^{\frac{1}{2}}\psi(\Pi_{\frac{1}{2}}). \quad (10)$$

$\psi(\Pi_{\frac{1}{2}})$ and $\psi(\Pi_{\frac{3}{2}})$ represent pure Hund's case (a) wave functions. In the double signs of (10) the upper ones apply to regular fine structure doublets (λ positive) and the lower to inverted doublets (λ negative). By letting $\lambda\to+\infty$ one sees from (10) that $\psi_{\text{Int. }1}$ and $\psi_{\text{Int. }2}$ denote those wave functions in the intermediate state that represent the pure $\Pi_{\frac{1}{2}}$ and $\Pi_{\frac{3}{2}}$ states respectively in the limit of Hund's case (a) of regular doublets. For inverted doublets this connection is reversed, i.e., for negative values of λ,

$$\psi_{\text{Int.}1}\to\psi(\Pi_{\frac{3}{2}}),\quad \psi_{\text{Int. }2}\to\psi(\Pi_{\frac{1}{2}}).$$

In the limit, Hund's case (b) ($2BJ\gg|A|$), the wave functions (10) will represent the two components of the spin doublet. In particular $\psi_{\text{Int. }1}$ and $\psi_{\text{Int. }2}$ go over to the states with $J=N+\frac{1}{2}$ and $J=N-\frac{1}{2}$ respectively. Expression (10) applies also to the lowest rotational level and properly expresses the fact that this state ($|J|=\frac{1}{2}$) is a pure $\psi(\Pi_{\frac{1}{2}})$ level. For $J=\frac{1}{2}$ $\psi_{\text{Int. }1}$ and $\psi_{\text{Int. }2}$ equal $\psi(\Pi_{\frac{1}{2}})$ for λ positive and negative respectively. As mentioned above, wave functions (10) will be used in evaluating the magnetic moment, hfs and line intensities. The effect of the Σ state which has been neglected in constructing (10) can be taken into account, when required in the calculation of these quantities, by second-order perturbation theory.

(b) Molecular Energies to Order $[(E_{\text{rot}}\text{ or }E_{\text{fs}})/E_{\text{el}}]^2$. Λ-Doubling in $^2\Pi$ and ρ-Doubling in $^2\Sigma$ States

The terms in first and second order in the expansion parameters that are to be considered arise from the interactions between the $^2\Pi$ and $^2\Sigma$ states. The most important effects of these interactions are the Λ-type doubling in the $^2\Pi$ states and the ρ-type doubling in the $^2\Sigma$ state.

These higher order terms are derived as follows: The determinant (5) is expanded and written in the form

$$\kappa\beta\gamma+\mu\epsilon\eta^*+\eta\mu^*\epsilon^*-\beta\eta\eta^*-\gamma\mu\mu^*-\kappa\epsilon\epsilon^*-(\kappa\beta+\kappa\gamma+\beta\gamma-\epsilon\epsilon^*-\mu\mu^*-\eta\eta^*)\lambda+(\kappa+\beta+\gamma)\lambda^2-\lambda^3=(\lambda-\lambda_1)(\lambda-\lambda_2)(\lambda-\lambda_3), \quad (11)$$

where

$$\lambda_i=\lambda_i{}^{(0)}+\lambda_i{}^{(1)},\quad i=1,2,3. \quad (12)$$

In (12) $\lambda_1{}^{(0)}$, $\lambda_2{}^{(0)}$, $\lambda_3{}^{(0)}$ are the zero-order solutions of (5):

$$\lambda_1{}^{(0)}=\kappa,\quad \lambda_{2,3}{}^{(0)}=\tfrac{1}{2}(\beta+\gamma\pm B_pX). \quad (13)$$

If the λ_i from (12) are introduced into (11) and terms higher than first-order in $\lambda_1{}^{(1)}$ or $1/E$ are omitted, three

[17] One may note that in expansion (6) the terms $(B/E)^0$, $(B/E)^1$, $(B/E)^2$ correspond to terms $(m/M)^1$, $(m/M)^2$, $(m/M)^3$, in Born-Oppenheimer approximation.

[18] G. Herzberg, *Molecular Spectra and Molecular Structure.* (D. Van Nostrand Company, Inc., New York, 1950), vol. 1.

linear equations for the unknowns $\lambda_i^{(1)}$ are obtained.

$$\lambda_1^{(1)}=(\mu\mu^*+\eta\eta^*)/E,$$

$$\lambda_{2,3}^{(1)}=-\frac{(\mu\mu^*+\eta\eta^*)}{2E}\mp\frac{1}{EB_pX}\Big[\frac{(\beta-\gamma)(\mu\mu^*-\eta\eta^*)}{2}+\mu\epsilon\eta^*+\mu^*\epsilon^*\eta\Big]. \quad (14)$$

The energies to this order had already been given[16] in terms of these matrix elements.

We carry out this procedure once more to obtain the next order terms. The derivation will be only briefly outlined here since it is rather straightforward, although tedious and lengthy. We write

$$\lambda_i=\lambda_i^{(0)}+\lambda_i^{(1)}+\lambda_i^{(2)}, \quad i=1, 2, 3 \quad (15)$$

$\lambda_i^{(0)}+\lambda_i^{(1)}$ is the sum of the zero and first order terms given by (13) and (14). Inserting (15) in (11) and equating coefficients of the same powers of λ on both sides, one obtains three cubics in the new unknowns $\lambda_i^{(2)}$. These become the following three linear equations when terms in powers of $\lambda_i^{(2)}$ higher than the first and those in $1/E$ higher than the second are omitted.

$$\lambda_1^{(2)}=\frac{1}{E^2}[\mu\mu^*\beta+\eta\eta^*\gamma+\mu\epsilon\eta^*+\eta\mu^*\epsilon^*-(\eta\eta^*+\mu\mu^*)(\alpha'+\delta)], \quad (16)$$

$$\lambda_{2,3}^{(2)}=\frac{\pm1}{E^2B_pX}\Big[(\mu\mu^*+\eta\eta^*)\Big(\frac{(\beta+\gamma)^2-B_p^2X^2}{4}\Big)-(\mu\mu^*\beta+\eta\eta^*\gamma+\mu\epsilon\eta^*+\eta\mu^*\epsilon^*)\Big(\frac{\beta+\gamma\pm B_pX}{2}\Big)-(\alpha'+\delta)(\beta\eta\eta^*+\gamma\mu\mu^*-\mu\epsilon\eta^*-\mu^*\epsilon^*\eta)+(\alpha'+\delta)(\eta\eta^*+\mu\mu^*)\Big(\frac{\beta+\gamma\pm B_pX}{2}\Big)+\frac{1}{B_p^2X^2}[(\beta-\gamma)^2\mu\mu^*\eta\eta^*+\epsilon\epsilon^*(\mu^2\mu^{*2}+\eta^2\eta^{*2})-2\mu\mu^*\eta\eta^*\epsilon\epsilon^*-(\beta-\gamma)(\mu\mu^*-\eta\eta^*)\times(\mu\epsilon\eta^*+\eta\mu^*\epsilon^*)]\Big]. \quad (17)$$

In Eqs. (13)–(17) where double signs occur the upper ones are to be taken for the $\Pi_{\frac{1}{2}}$ state and the lower for the $\Pi_{\frac{3}{2}}$ state in inverted doublets. In regular doublets the upper signs apply to the $\Pi_{\frac{3}{2}}$ state and the lower to the $\Pi_{\frac{1}{2}}$ state.

The energies then, to second order, are the sum

$$\lambda_i^{(0)}+\lambda_i^{(1)}+\lambda_i^{(2)}.$$

The λ_i given above represents only one component of the Λ-type doublet in each Π state and given J. The energy of the other is given by the same expressions except that δ is replaced by $-\delta$ and ζ by $-\zeta$.

The energy expressions involve the molecular constants $E(\equiv E_\Sigma-E_\Pi)$, B_p, B_s, $\lambda(\equiv A/B_p)$ and the following two products of specific matrix elements connecting the $^2\Pi$ with the $^2\Sigma$ state:

$$\langle\Pi|AL_y+2BL_y|\Sigma\rangle\langle\Sigma|BL_y|\Pi\rangle$$

and

$$|\langle\Pi|BL_y|\Sigma\rangle|^2.$$

One considers the quantities

$$\alpha_p\equiv4\sum_{\Sigma\text{-states}}(-1)^s\frac{\langle\Pi|AL_y+2BL_y|\Sigma\rangle\langle\Sigma|BL_y|\Pi\rangle}{E_\Sigma-E_\Pi},$$
$$\beta_p\equiv4\sum_{\Sigma\text{-states}}(-1)^s\frac{|\langle\Pi|BL_y|\Sigma\rangle|^2}{E_\Sigma-E_\Pi} \quad (18)$$

as additional molecular parameters that measure the effects of $^2\Sigma$ states on the $^2\Pi$ state. The summation over Σ states in (18) is to indicate that the interactions of all Σ states with the $^2\Pi$ are taken into account.

The interaction with the $^2\Sigma$ state produces a shift in the energy of each J level in the $^2\Pi$ states and in addition splits it into the Λ-type doublet. We write then for the energy of a level with given J:

$$W=W_1\pm\tfrac{1}{2}W_2, \quad (19)$$

where W_2 represents the splitting of the Λ-type doublet.

Explicit expressions for W in terms of J and the molecular constants can be obtained from Eqs. (13), (14), and (17) using the matrix elements listed in Appendix II. They are

$$W_1=B_p'(J-\tfrac12)(J+\tfrac32)\pm\frac{B_p''X}{2}+C_1\mp\frac{\alpha_p}{X}\Big[(J-\tfrac12)(J+\tfrac32)\Big(1+\frac{B_p}{E}(J-\tfrac12)(J+\tfrac32)-\frac{B_s}{E}(J+\tfrac12)^2\Big)-\Big(\frac{2-\lambda}{2}\Big)\frac{B_s}{E}(J+\tfrac12)^2\Big]\mp\frac{\beta_p}{2X}\Big[(2-\lambda)\Big(1+\frac{B_p}{E}(J-\tfrac12)(J+\tfrac32)-\frac{B_s}{E}(J+\tfrac12)^2\Big)+\frac{B_pX^2}{E}J(J+1)-\frac{4B_s}{E}(J+\tfrac12)^2(J-\tfrac12)(J+\tfrac32)\Big]\mp\frac{\alpha_p^2}{8\beta_p}\Big(\frac{2-\lambda}{X}\Big)\Big[1+\frac{B_p}{E}(J-\tfrac12)(J+\tfrac32)-\frac{B_s}{E}(J+\tfrac12)^2\Big]\pm\frac{(J-\tfrac12)(J+\tfrac32)}{B_pX^3}\Big[\alpha_p^2\Big(\Big(\frac{2-\lambda}{2}\Big)^2+J(J+1)+\tfrac34\Big)+\beta_p^2(J+\tfrac12)^2[(2-\lambda)^2+1]-2\alpha_p\beta_p(2-\lambda)\times[J(J+1)+\tfrac34]+\frac{\alpha_p^4}{16\beta_p^2}-\frac{\alpha_p^3(2-\lambda)}{4\beta_p}\Big]-\frac{\beta_p(B_p-B_s)}{E}J^2(J+1)^2, \quad (20)$$

where

$$B_p'=B_p-\beta_p\left(1-\frac{B_p}{E}\right)-\alpha_p\left(1+\frac{\alpha_p}{4\beta_p}\right)\left(\frac{B_p-B_s}{2E}\right),$$

$$B_p''=B_p\left(1-\frac{\alpha_p^2-2\beta_p^2}{8\beta_pE}\right),$$

$$C_1=-\frac{\alpha_p^2}{8\beta_p}\left(1-\frac{\lambda B_p}{2E}+\frac{B_p-B_s}{E}\right)-\frac{1}{2}\beta_p\left(1+\frac{\lambda B_p}{2E}-\frac{B_p-B_s}{8E}\right)+\frac{\alpha_pB_s}{2E}.$$

(One may add to C_1 the term $B_p(L_x^2+L_y^2)$ that was neglected earlier.) Denoting the first- and second-order contributions to W_2 as $\nu_\Lambda^{(1)}$ and $\nu_\Lambda^{(2)}$ one obtains

$$W_2=\nu_\Lambda^{(1)}+\nu_\Lambda^{(2)}, \tag{21}$$

$$\nu_\Lambda^{(1)}=-\alpha_p(J+\tfrac{1}{2})\left(\frac{\pm X+2-\lambda}{\pm X}\right)\mp\frac{4\beta_p}{X}(J-\tfrac{1}{2})\times(J+\tfrac{1}{2})(J+\tfrac{3}{2}), \tag{22}$$

$$\nu_\Lambda^{(2)}=\pm\frac{(J+\frac{1}{2})}{EX}\alpha_p\Big[(2(J-\tfrac{1}{2})(J+\tfrac{3}{2})\pm X)\Big((B_s-B_p)(J+\tfrac{1}{2})^2+B_p\Big(\frac{\lambda\mp X}{2}+(J-\tfrac{1}{2})(J+\tfrac{3}{2})\Big)\Big)$$

$$-2B_s((J+\tfrac{1}{2})^2(J(J+1)-7/4+\lambda/2)-(J-\tfrac{1}{2})(J+\tfrac{3}{2}))\Big]\pm\frac{(J+\frac{1}{2})}{EX}\beta_p[(2(J-\tfrac{1}{2})(J+\tfrac{3}{2})\pm X)$$

$$\times(2B_s(J(J+1)-\tfrac{1}{4})-2B_p(J-\tfrac{1}{2})(J+\tfrac{3}{2}))+B_s(2(J+\tfrac{1}{2})^2-\lambda)]$$

$$\mp\frac{(J+\frac{1}{2})}{EX}\frac{\alpha_p^2}{4\beta_p}B_s(\lambda-2\mp X)\mp\frac{C_2(J-\frac{1}{2})(J+\frac{1}{2})(J+\frac{3}{2})}{B_pX^3}, \tag{23}$$

where

$$C_2=-2\alpha_p\beta_p(\lambda^2-4\lambda+6)+(3\alpha_p^2+4\beta_p^2)(2-\lambda)-\alpha_p^3/\beta_p.$$

In (20), (22), and (23) the upper signs apply to the $\Pi_{\frac{3}{2}}$ states of regular doublets and the $\Pi_{\frac{1}{2}}$ states of inverted ones. The lower signs are to be taken for the $\Pi_{\frac{1}{2}}$ state of regular and the $\Pi_{\frac{3}{2}}$ state of inverted doublets. For molecules close to Hund's case (*b*) the upper and lower signs apply to states with $N=J+\frac{1}{2}$ and $N=J-\frac{1}{2}$, respectively.

The terms in first and second order in expansion parameters appear above in a somewhat disguised form. First order terms are directly proportional to α_p, β_p or α_p^2/β_p, whereas the ones in second order have denominators E or B_pX^3.

The energy expressions given above do not contain terms due to the interaction between the electron magnetic moment and magnetic fields generated directly by the rotation of the nuclei. Such terms have the form $\gamma\mathbf{N}\cdot\mathbf{S}$. These small effects are not easily separated from the ones due to the $^2\Pi-{}^2\Sigma$ interaction. The $\gamma\mathbf{N}\cdot\mathbf{S}$ interaction may be explicitly introduced in the Hamiltonian. One then should add the constant term $-\gamma/2$ to the energies of $\Pi_{\frac{1}{2}}$ and $\Pi_{\frac{3}{2}}$ states and replace in the intermediate coupling formulas λ by $\lambda+\gamma/B_p$ and X approximately by

$$X'\equiv[4(J+\tfrac{1}{2})^2(1-\gamma/2B_p)^2+\lambda(\lambda-4)+2\lambda\gamma/B_p]^{\frac{1}{2}}.$$

γ is of order $(m/M)A$, and hence much smaller than either A or B. In the $^2\Sigma$ state this interaction will, in addition, contribute directly to the ρ-type doubling as will be discussed below.

We will discuss here the Λ-type doubling in some detail. The energy expressions given above apply in the general coupling scheme intermediate between Hund's cases (*a*) and (*b*). Simplified forms of the first order term $\nu_\Lambda^{(1)}$ for the pure cases (*a*) or (*b*) can be obtained. However, if one uses the second order term $\nu_{\Lambda 1}^{(2)}$, the general formula (22) should be used for $\nu_\Lambda^{(1)}$ rather than any limiting case form since the effects of intermediate coupling are almost always larger than the correction $\nu_\Lambda^{(2)}$.

On the other hand, along with the general formula (22) for $\nu_\Lambda^{(1)}$ one can use, for molecules extremely close to pure coupling scheme, simplified forms of $\nu_\Lambda^{(2)}$. From (23), letting $\lambda\rightarrow\pm\infty$, one derives for pure Hund's case (*a*) ($|A|\gg 2BJ$) for $\Pi_{\frac{1}{2}}$ states:

$$\nu_\Lambda^{(2)}=\mp\left(\frac{\alpha_p-2\beta_p}{2E}\right)\left(|A|-\frac{B_s(\alpha_p-2\beta_p)}{\beta_p}\right)(J+\tfrac{1}{2}), \tag{24}$$

and for $\Pi_{\frac{3}{2}}$ states

$$\nu_\Lambda^{(2)}=\pm\left(\frac{\alpha_p-2\beta_p}{2E}\right)(|A|)(J+\tfrac{1}{2}). \tag{25}$$

In (24) and (25) the upper and lower signs apply to inverted and regular doublets respectively. In deriving these formulas terms of the form AB^2/E^2 and B^3/E^2 have been neglected as small compared to A^2B/E^2.

For the limiting case (*b*) ($2BJ\gg|A|$) from (23)

letting $\lambda\to 0$

$$\nu_\Lambda^{(2)}=\pm\frac{2(B_s-B_p)}{E}\beta_p[J^2(J+1)^2\pm J(J+1)(2J+1)+\tfrac{1}{2}J(J+1)+\tfrac{3}{16}]\pm\frac{B_s+B_p}{E}\beta_p[2J(J+1)+\tfrac{1}{4}\pm 1]. \quad (26)$$

The upper and lower signs apply to states with $N=J+\frac{1}{2}$ and $N=J-\frac{1}{2}$ respectively. Again in deriving (26) only terms of the form B^3/E^2 have been retained, the terms A^2B/E^2 and AB^2/E^2 being neglected. Hence (26) and also (24), (25) should hold only for cases very close to the pure coupling schemes. For cases such as the OH where $|A|\sim 2BJ$ the general formula (23) has to be applied.

In the $^2\Sigma$ state for each rotational level with rotational angular momentum quantum number N there are two states that correspond to the two orientations of **S** relative to **N**. The energies are the sum $\lambda_1^{(0)}+\lambda_1^{(1)}+\lambda_1^{(2)}$ given by (13), (14), and (16). Corresponding to $J=N\mp\frac{1}{2}$, one takes in these expressions $\kappa=\alpha\pm(-1)^S\delta$ and $\mu=\theta\pm(-1)^S\zeta$. Thus for levels of the same N:

$$W_\Sigma=C_3+B_s'N(N+1)\pm\left[\alpha_s\left(1-\frac{\lambda B_p}{2E}\right)-2\beta_s\left(1-\frac{B_p}{2E}\right)-\frac{\alpha_s^2B_p}{4\beta_sE}\right](N+\tfrac{1}{2})\pm(\alpha_s-2\beta_s)\left(\frac{B_p-B_s}{E}\right)N(N+1)(N+\tfrac{1}{2})+2\beta_s\left(\frac{B_p-B_s}{E}\right)N^2(N+1)^2, \quad (27)$$

where

$$C_3=E-\frac{\alpha_s}{2}\left[1+\left(\frac{4-\lambda}{2}\right)\frac{B_p}{E}\right]+\frac{\beta_sB_p}{2E}(3-\lambda)+\frac{\alpha_s^2}{4\beta_s}\left(1+\left(\frac{1-\lambda}{2}\right)\frac{B_p}{E}\right),$$

and

$$B_s'=B_s+2\beta_s\left(1-\frac{B_p}{E}\right)-\alpha_s\left(\frac{B_p-B_s}{2E}\right)+\frac{\alpha_s^2}{4\beta_s}\left(\frac{B_p+B_s}{E}\right).$$

The constants α_s, β_s are defined as

$$\alpha_s\equiv 4\sum_{\Pi\text{-states}}(-1)^s\frac{\langle\Pi|AL_y+2BL_y|\Sigma\rangle\langle\Sigma|BL_y|\Pi\rangle}{E_\Sigma-E_\Pi},$$
$$\beta_s\equiv 4\sum_{\Pi\text{-states}}(-1)^s\frac{|\langle\Pi|BL_y|\Sigma\rangle|^2}{E_\Sigma-E_\Pi}, \quad (28)$$

and differ from α_p and β_p only in that the summation is over all Π instead of over all Σ states. If only one Π state interacts with one Σ state then $\alpha_p=\alpha_s$, $\beta_p=\beta_s$. The upper and lower signs in (27) apply to the states with $J=N-\frac{1}{2}$ and $J=N+\frac{1}{2}$ respectively.

The energy difference between these two states gives the ρ-type doubling:

$$\nu_\rho=2\left[\alpha\left(1-\frac{\lambda B_p}{2E}\right)-2\beta_s\left(1-\frac{B_p}{2E}\right)-\frac{\alpha_s^2B_p}{4\beta_sE}\right](N+\tfrac{1}{2})+(\alpha_s-2\beta_s)\left(\frac{B_p-B_s}{E}\right)N(N+1)(2N+1). \quad (29)$$

One sees from (29) that when the magnetic interaction constant A is zero, $\alpha_s=2\beta_s$ and both first- and second-order contributions to ν_ρ vanish. Hence in this case the interaction with the $^2\Pi$ state (L-uncoupling) does not remove the degeneracy of the levels with $J=N\pm\frac{1}{2}$ in $^2\Sigma$ state. The degeneracy however can be removed directly by magnetic fields generated by the rotation of the nuclei themselves rather than the transfer of rotational angular momentum to the electrons. The direct interaction ($\mathbf{N}\cdot\mathbf{S}$) produces a splitting

$$\nu_\rho'=\text{const}(N+\tfrac{1}{2}),$$

which is of the same form as the first term of (29).

Certain points concerning the form of the energy expressions for the $^2\Pi$ and $^2\Sigma$ states should be noted. The inclusion of effects in second order does not introduce any new parameters. α_p, β_p and the similar quantities α_s and β_s suffice to describe the $^2\Pi-{}^2\Sigma$ interactions to both first and second order in expansion parameters.[19] Part, but not all, of the first and second order terms (aside from the ones that contribute to doubling) have the J or N dependence of the usual rotational energy terms. The effect of these terms appears as a contribution to that due to the "bona fide" moment of inertia. However, only a part of the higher order terms can be accounted for by expressions like $B_{\text{effective}}J(J+1)$. There are also terms of the form $J^2(J+1)^2$ or $N^2(N+1)^2$ which will add to the usual centrifugal distortion term.

The relative order of magnitude of the first and second order terms can be readily established by comparing, for instance, the two contributions $\nu_\Lambda^{(1)}$ and $\nu_\Lambda^{(2)}$ to the Λ-type doubling. Inserting approximate numerical values in (22) and (23) above for OH, one sees that

$$\nu_\Lambda^{(2)}\sim(1/350)\nu_\Lambda^{(1)},$$

which is of the order to be expected from the values (1/234) and (1/1726) of our expansion parameters.

From this result one might surmise that the energy

[19] *Note added in proof.*—The constants α^2, β^2 that appear in some of the second-order terms are strictly the squares of the first-order constants α and β only in the approximation of one Π state interacting with one or several closely spaced Σ states.

expressions given above should account for the $^2\Pi-^2\Sigma$ interactions to about one part in 100 000 which is comparable to the experimental accuracy. There are, however, substantial corrections to be applied to these formulas. The most important one, which also can be readily taken into account, is the effect of centrifugal distortion on the moment of inertia. In addition to B this would affect λ and also α_p, β_p, α_s, β_s.

The rotational constant may be written

$$B=B_0\left[1-\frac{D_0}{B_0}f(N \text{ or } J)\right],$$

where D_0 is the centrifugal distortion constant $(=4B^3/\omega_{\text{vib}}^2)$. In $^2\Sigma$ states and also in the limiting Hund's case (b) for $^2\Pi$ states, $f(N)$ is $N(N+1)$. We will use here a more elaborate form, derived in Sec. 4f, which applies to intermediate coupling states. λ then has the form

$$\lambda=\lambda_0\left(1+\frac{D_0}{B_0}f\right),$$

and in quantities such as α_p,

$$\langle\Pi|BL_y|\Sigma\rangle = (\langle\Pi|BL_y|\Sigma\rangle)_0\left(1-\frac{D_0}{B_0}f\right). \quad (30)$$

Expression (30) implies the separation of B from the rest of the matrix element (pure precession hypothesis, only approximately correct), but only for the centrifugal correction on B. For the main contribution to the energies the constants to be determined from the data, defined in (18) and (28) above, are quite independent of this restriction.

When one strives for theoretical accuracy comparable to that of the data, the question arises whether the constants α_p, β_p, α_s, β_s are independent of small changes in internuclear distance (aside from the direct effect on B) that result from centrifugal stretching. A small change of the wave function from one rotational state to the next, affecting the matrix $\langle\Pi|L_y|\Sigma\rangle$ is not unexpected in extremely light molecules such as the OH. Such a variation is indicated by the experimental data and is discussed, along with some other small contributions to the energies, in Sec. 5(a).

(c) Magnetic Hyperfine Structure

The magnetic hyperfine structure may be considered to arise from (a) the interaction $(\mathbf{I}\cdot\mathbf{L})$ of the nuclear magnetic moment with the orbital motion of the unpaired electron or electrons (b) the dipole-dipole interaction $\mathbf{I}\cdot\mathbf{S}/r^3-3(\mathbf{I}\cdot\mathbf{r})(\mathbf{S}\cdot\mathbf{r})/r^5$ and (c) the relativistic part of the spin-spin interaction that is characteristic of atomic s-states.

The theory of magnetic hyperfine structure in diatomic molecules has been given by Frosch and Foley,[20] who derived the Hamiltonian from the Dirac equation for the electron. An alternative and simplified derivation of the hyperfine interaction, along the lines indicated in the preceding paragraph, has also been given.[21] This recent re-examination of the theory has revealed that two constants (denoted below by d and e) in the Hamiltonian of Frosch and Foley need be corrected by numerical factors of two. Aside from this the Hamiltonian is that of Frosch and Foley. Thus

$$H_2=a\mathbf{I}\cdot\mathbf{L}+(b+c)I_zS_z+\tfrac{1}{2}b(I^+S^-+I^-S^+) +\tfrac{1}{2}d(e^{2i\varphi}I^-S^-+e^{-2i\varphi}I^+S^+) +e[e^{i\varphi}(S^-I_z+I^-S_z)+e^{-i\varphi}(S^+I_z+I^+S_z)], \quad (31)$$

where

$$I^+=I_x+iI_y, \quad I^-=I_x-iI_y, \quad \text{etc.},$$

$$a=2\mu_0\frac{\mu_I}{I}(1/r^3)_{\text{Av}},$$

$$b=-\mu_0\frac{\mu_I}{I}[(3\cos^2\chi-1)/r^3]_{\text{Av}}+\frac{16\pi}{3}\mu_0\frac{\mu_I}{I}\psi^2(0),$$

$$c=3\mu_0\frac{\mu_I}{I}[(3\cos^2\chi-1)/r^3]_{\text{Av}},$$

$$d=3\mu_0\frac{\mu_I}{I}(\sin^2\chi/r^3)_{\text{Av}},$$

$$e=3\mu_0\frac{\mu_I}{I}(\sin\chi\cos\chi/r^3)_{\text{Av}}.$$

μ_0 is the Bohr magneton (taken as positive) and μ_I and I are the nuclear magnetic moment and spin respectively. $\mathbf{r}$ denotes the radius vector from the nucleus to the interacting electron and χ the angle between $\mathbf{r}$ and the internuclear axis. The angle φ is defined through the relations $x=r\sin\chi\cos\varphi$, $y=r\sin\chi\sin\varphi$, hence the φ dependence of the wave function is $e^{\pm i\Lambda\varphi}$. $\psi^2(0)$ is the probability density of electron spin at the nucleus whose hyperfine interaction is being considered.

The averages are to be taken only over the electron or electrons that contribute to the hyperfine interaction. In particular, the average involved in the constant a is to be taken over the electron(s) possessing unpaired orbital angular momentum, whereas the constants b, c, d, and e are associated with electron(s) carrying unpaired spins. The terms aI_zL_z and $(b+c)I_zS_z$ in (31) have matrix elements diagonal in Λ and Σ and give the same energy contributions to each member of the Λ-type doublet. The operator

$$d(e^{2i\varphi}I^-S^-+e^{-2i\varphi}I^+S^+)/2$$

[20] R. A. Frosch and H. M. Foley, Phys. Rev. 88, 1347 (1952).
[21] G. C. Dousmanis, Phys. Rev. 97, 967 (1955).

has matrix elements of the form $\Delta\Lambda=\pm 2$ and for specific values of Λ and Σ gives equal and opposite contributions to each member of the Λ doublet.[22]

The matrix elements of H_2 are written down in a pure Hund's case (a) representation, using the relation[23]:

$$\langle \alpha J|I^i|\alpha' J\rangle=\langle \alpha J|J^i|\alpha' J\rangle \mathbf{I}\cdot\mathbf{J}/J(J+1)$$

for matrix elements diagonal in J.

Thus

$$\begin{aligned}\langle \Pi_{\frac{1}{2}}|H_2|\Pi_{\frac{1}{2}}\rangle&=\tfrac{1}{2}[a-\tfrac{1}{2}(b+c)]\mathbf{I}\cdot\mathbf{J}/J(J+1)\\&\qquad\pm\tfrac{1}{2}d(J+\tfrac{1}{2})\mathbf{I}\cdot\mathbf{J}/J(J+1),\\\langle \Pi_{\frac{3}{2}}|H_2|\Pi_{\frac{3}{2}}\rangle&=\tfrac{3}{2}[a+\tfrac{1}{2}(b+c)]\mathbf{I}\cdot\mathbf{J}/J(J+1),\\\langle \Pi_{\frac{1}{2}}|H_2|\Pi_{\frac{3}{2}}\rangle&=-\tfrac{1}{2}b[(J-\tfrac{1}{2})(J+\tfrac{3}{2})]^{\frac{1}{2}}\mathbf{I}\cdot\mathbf{J}/J(J+1).\end{aligned}\tag{32}$$

The hyperfine energies are evaluated from these matrix elements and the wave functions given in (10) above. For the general coupling case intermediate between (a) and (b)

$$\begin{aligned}W_{\rm hfs}=\frac{1}{\pm 4X}\Big[&2a(\pm 2X+2-\lambda)\\&+b(4(J-\tfrac{1}{2})(J+\tfrac{3}{2})\pm X+4-2\lambda)\\&+c(\pm X+4-2\lambda)\Big]\frac{\mathbf{I}\cdot\mathbf{J}}{J(J+1)}\\&\pm\frac{d}{2}\left(\frac{\pm X-2+\lambda}{\pm 2X}\right)\left(\frac{(J+\tfrac{1}{2})\mathbf{I}\cdot\mathbf{J}}{J(J+1)}\right).\end{aligned}\tag{33}$$

The double signs in (33) need elaborate explanation. The positive sign in front of X applies to states that go over to the pure $\Pi_{\frac{1}{2}}$ state of Hund's case (a) for regular fine structure doublets or the $\Pi_{\frac{3}{2}}$ state in inverted doublets. For states close to case (b), the positive sign applies to that state that goes over to the $J=N+\frac{1}{2}$ member of the spin doublet. The negative sign in front of X is to be taken with states that are connected in case (a) with the $\Pi_{\frac{3}{2}}$ state for regular doublets or the $\Pi_{\frac{1}{2}}$ state for inverted ones, and in Hund's case (b) with the state $J=N-\frac{1}{2}$.

The terms of (33) proportional to a, b and c give identical hyperfine structure for each member of the Λ doublet. Superimposed on this structure appears the "hyperfine doubling" term in d which gives equal and opposite contributions to each member of the Λ doublet. The positive sign in front of d applies to the upper and the negative to the lower Λ-doublet level in $\Pi_{\frac{1}{2}}$ states in case (a) and the state with $J=N+\frac{1}{2}$ case (b). The signs are the reverse in case (b) for the state $J=N-\frac{1}{2}$. The term in d vanishes for $\Pi_{\frac{3}{2}}$ states in case (a).

[22] For a detailed description of this "hyperfine doubling" see reference 9.

[23] E. U. Condon and G. H. Shortley, *The Theory of Atomic Spectra* (Cambridge University Press, Cambridge, 1953), p. 61.

Simplified expressions for $W_{\rm hfs}$ that apply in the limiting cases can be derived from (33) by letting $\lambda\to\pm\infty$ or $\lambda\to 0$. These special formulas have been given elsewhere.[9]

Certain second-order effects have been neglected in deriving (33). These are due to cross terms between molecular (H_1) and hyperfine operators (H_2) with matrix elements of the form $\Delta\Lambda=\pm 1$, which connect $^2\Pi$ and $^2\Sigma$ states. These effects are very similar to the $C\mathbf{I}\cdot\mathbf{J}$ interactions in $^1\Sigma$ molecules. Their approximate magnitude is

$$\frac{A}{E_\Sigma-E_\Pi}\cdot W_{\rm hfs}\quad\text{or}\quad\frac{BJ}{E_\Sigma-E_\Pi}\cdot W_{\rm hfs}$$

or for OH about 0.4 Mc/sec. These effects then would give contributions somewhat larger than our experimental error, but not substantial enough to warrant quantitative determination from the present data. Terms of the form $W_{\rm hfs}^2/(E_\Sigma-E_\Pi)$, $W_{\rm hfs}^2/(E_{\Pi_{\frac{1}{2}}}-E_{\Pi_{\frac{3}{2}}})$ and $W_{\rm hfs}^2/E_{\rm rot}$ are smaller than the experimental error by an order of magnitude.

(d) Molecular Magnetic Moment and Zeeman Effect

The effects of intermediate coupling manifest themselves rather prominently in the molecular magnetic moment. In a Hund's case (a) coupling scheme both $\mathbf{L}$ and $\mathbf{S}$ are quantized along the internuclear axis. The magnetic moment in the $\Pi_{\frac{3}{2}}$ state would be rather large (about two Bohr magnetons) whereas it would be close to zero in the $\Pi_{\frac{1}{2}}$ state. An increasing amount of end-over-end rotation of the nuclei gradually decouples the spin from the axis and the $\Pi_{\frac{1}{2}}$ state gains thereby magnetic moment at the expense of the $\Pi_{\frac{3}{2}}$ state. The extent of spin uncoupling for given J depends exclusively on the relative values of the spin-orbit coupling constant A and the rotational constant B.

Quantitatively, the magnetic moment operator $(-\mu_0)(\mathbf{L}+2\mathbf{S})$ is evaluated in the appropriate intermediate coupling eigenstate represented by the wave functions (10) above. We assume that the applied magnetic fields are too small (as is our case) to influence the molecular coupling. The matrix elements are

$$\begin{aligned}&\langle \Pi_{\frac{1}{2}}|\mu_J|\Pi_{\frac{1}{2}}\rangle=0,\\&\langle \Pi_{\frac{3}{2}}|\mu_J|\Pi_{\frac{3}{2}}\rangle=-3\mu_0/[J(J+1)]^{\frac{1}{2}},\\&\langle \Pi_{\frac{1}{2}}|\mu_J|\Pi_{\frac{3}{2}}\rangle=\mu_0[(J-\tfrac{1}{2})(J+\tfrac{3}{2})/J(J+1)]^{\frac{1}{2}}.\end{aligned}$$

From above and (10) the magnetic moment is obtained as

$$\mu_J=-\frac{\mu_0}{[J(J+1)]^{\frac{1}{2}}}\left(\frac{3}{2}\pm\frac{2(J-\tfrac{1}{2})(J+\tfrac{3}{2})-\tfrac{3}{2}\lambda+3}{[4(J+\tfrac{1}{2})^2+\lambda(\lambda-4)]^{\frac{1}{2}}}\right).\tag{34}$$

In the double sign of (34), the positive one applies to $\Pi_{\frac{1}{2}}$ states of regular and $\Pi_{\frac{3}{2}}$ states of inverted doublets in Hund's case (a) and to the state with $J=N+\frac{1}{2}$ in

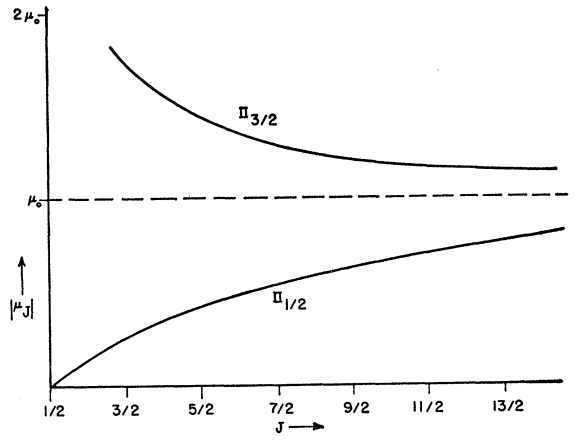

FIG. 3. The magnetic moment of OH as a function of J (from theory). Intermediate coupling introduces increasing amounts of magnetic moment into the $\Pi_{\frac{1}{2}}$ state. Neglected effects of the $^2\Sigma$ state and the anomalous moment of the electron would give small contributions (of order 0.001 μ_0) to all rotational states.

case (b). The negative sign applies to all other cases. μ_0 is taken as positive. This result can also be obtained by expanding, in the zero-field limit, the general formulas for the Zeeman effect given by Hill.[24]

The effects of the $^2\Sigma$ state are neglected. To this approximation both members of the Λ-type doublet have identical magnetic moments given by (34). A more detailed calculation should take into account the anomalous moment of the electron and the influence of the $^2\Sigma$ state. Both of these effects are of the same order of magnitude ($\sim 0.001\mu_0$) and much smaller than the contributions from intermediate coupling, except for the lowest rotational level $J=\frac{1}{2}$ in $\Pi_{\frac{1}{2}}$ states where the intermediate coupling effect vanishes. In pure case (a), for $\Pi_{\frac{3}{2}}$ states, (34) becomes

$$\mu_J=\frac{-3\mu_0}{[J(J+1)]^{\frac{1}{2}}}; \tag{35}$$

and in case (b),

$$\mu_J=\frac{-\mu_0}{[J(J+1)]^{\frac{1}{2}}}\left(\tfrac{3}{2}\pm(J+\tfrac{1}{2})\pm\frac{1}{2J+1}\right); \tag{36}$$

and for extremely high rotational states $\mu_J\rightarrow\pm\mu_0$ as one would expect, since $\mathbf{\Lambda}$ is perpendicular and $\mathbf{S}$ parallel or antiparallel to $\mathbf{J}$.

The behavior of μ_J in OH ($\lambda=-7.44$) as a function of J as given by (34) is shown in Fig. 3. The rise of the magnetic moment with J in the $\Pi_{\frac{1}{2}}$ state, and a value already of $0.3\mu_0$ for $J=\frac{3}{2}$, demonstrates that substantial Zeeman splittings can be obtained with fields of only a few gauss, which allows convenient detection of the spectra by Zeeman modulation.

At low fields that do not disturb the coupling scheme, and if nuclear spin is neglected for the moment, the Zeeman energies are

$$W_3=-\boldsymbol{\mu}\cdot\mathbf{H}=g_J\mu_0HM_J. \tag{37}$$

The molecular g-factor g_J is given by dividing the expressions for μ_J by $(-\mu_0)[J(J+1)]^{\frac{1}{2}}$.

When the hyperfine structure is much larger than the Zeeman energy, Zeeman effects in the presence of hyperfine structure can easily be calculated. Approximate numerical comparison of (33) with (37) ($H\sim 5$ gauss) shows that this is the case in the $\Pi_{\frac{1}{2}}$ state of both OH and OD and the $\Pi_{\frac{3}{2}}$ state of OH. In these states

$$W_3'=g_F\mu_0HM_F,$$
$$g_F=g_J\frac{F(F+1)+J(J+1)-I(I+1)}{2F(F+1)}. \tag{38}$$

The small term $\boldsymbol{\mu}_I\cdot\mathbf{H}$ is neglected in (38). For the $\Pi_{\frac{3}{2}}$ state in OD, (33) and (37) show that the hyperfine structure and the Zeeman effect are of the same order. This case requires more detailed treatment.[9] In the present work the Zeeman effect was used exclusively for detection purposes and precise measurements of it were not attempted.

(e) Matrix Element for Λ-Type Doubling Transitions in Intermediate Coupling

We are interested in the matrix element for electric dipole transitions of the type $\Delta J=0$ between the two members of the Λ doublet. The quantity that need be evaluated is

$$\langle\alpha J|\mu\mathbf{k}|\alpha' J\rangle,$$

where α and α' stand for the two states of the symmetric and antisymmetric type given by (4) above, μ is the electric dipole moment and $\mathbf{k}$ a unit vector along the internuclear axis.

In pure case (a) the matrix element is[9]

$$|\mu_{ij}|=\mu\Omega/[(J+1)(2J+1)]^{\frac{1}{2}}.$$

We use wave functions (10) to evaluate this in intermediate coupling. Since the electric dipole moment operator has no matrix elements connecting the $\Pi_{\frac{1}{2}}$ and $\Pi_{\frac{3}{2}}$ states, μ_{ij} is simply the sum of the contributions from the two pure components in each of the wave functions (10). Hence

$$|\mu_{ij}|^2=\frac{\mu^2}{(J+1)(2J+1)4X^2}[\Omega_1^2(\pm X-2+\lambda)^2$$
$$+\Omega_2^2(\pm X+2-\lambda)^2+2\Omega_1\Omega_2(X^2-(2-\lambda)^2)]. \tag{39}$$

With $\Omega_1=\frac{1}{2}$ and $\Omega_2=\frac{3}{2}$ in (39), the upper signs in front of X are to be taken for the state $J=N+\frac{1}{2}$ in case (b) or in case (a) for the $\Pi_{\frac{1}{2}}$ state when λ is positive and for the $\Pi_{\frac{3}{2}}$ state when λ is negative. The lower signs apply to the state which gives $J=N-\frac{1}{2}$ in case (b), or to the

[24] E. L. Hill, Phys. Rev. 34, 1507 (1929).

$^2\Pi_{\frac{3}{2}}$ or $^2\Pi_{\frac{1}{2}}$ state in case (*a*) if λ is positive or negative respectively.

In the limit of pure case (*b*), we can neglect $(2-\lambda)$ compared to X and (39) becomes

$$|\mu_{ij}|^2=\frac{\mu^2}{(J+1)(2J+1)}\left(\frac{\Omega_1+\Omega_2}{2}\right)^2=\frac{\mu^2\Lambda^2}{(J+1)(2J+1)}. \tag{40}$$

This expression applies to both components of the spin doublet, and is identical with the one for *l*-type doublet transitions in linear triatomic molecules.[9]

The main feature of the intermediate coupling formula (39) is that $|\mu_{ij}|^2$ in case (*a*) is 9 times stronger (for the same J) for the $^2\Pi_{\frac{3}{2}}$ state than for the $^2\Pi_{\frac{1}{2}}$ state. During the transition from case (*a*) to (*b*) the ratio $|\mu_{ij}|^2$ in $^2\Pi_{\frac{3}{2}}$ to that in $^2\Pi_{\frac{1}{2}}$ state gradually decreases until it becomes unity in case (*b*).

Expression (39) is the appropriate one to be substituted into (1) for the calculation of line intensities.

(f) Centrifugal Distortion in Intermediate Coupling

Effects of centrifugal distortion for a light molecule such as the OH represent substantial corrections that have to be applied to all expressions involving the rotational constant B. One uses

$$B=B_0\left(1-\frac{D_0}{B_0}f\right), \tag{41}$$

where D_0 is the centrifugal constant and f has the form $N(N+1)$ in pure case (*b*).

We need the form of f that applies in the intermediate coupling state. One can see that the distortion will depend on the extent of intermediate coupling from the following simple consideration. In pure case (*b*) the distortion depends exclusively on N, which fails to be a good quantum number when the perturbation $A\mathbf{L}\cdot\mathbf{S}$, with matrix elements $\Delta N=\pm1$, introduces intermediate coupling.

One can calculate f in the general case starting with basic wave functions of case (*a*) [(10) above] or case (*b*). It is probably more appropriate to use for this correction basic wave functions of Hund's case (*b*), since in OH the value of D_0 has been obtained from ultraviolet measurements[3] involving higher rotational states and using the form $N(N+1)$. We will then calculate this distortion starting with the case (*b*) representation, where the fine structure rather than the rotational energy is considered as a perturbation. To obtain the required intermediate wave functions the matrix

$$\begin{array}{c} \\ N=J+\frac{1}{2} \\ N=J-\frac{1}{2} \end{array}\begin{array}{c} \begin{array}{cc} N=J+\frac{1}{2} & N=J-\frac{1}{2} \end{array} \\ \begin{pmatrix} H_{11} & H_{12} \\ H_{21} & H_{22} \end{pmatrix} \end{array} \tag{42}$$

need to be diagonalized. The matrix elements are[25]

$$H_{11}=B[(J+\tfrac{1}{2})^2+J-\tfrac{1}{2}]-A/(2J+1),$$
$$H_{22}=B[(J^2-\tfrac{1}{4})-1]+A/(2J+1),$$
$$H_{12}=A[(J+\tfrac{1}{2})^2-1]^{\frac{1}{2}}/(2J+1).$$

(42) of course yields the same energies (8) that were obtained on the basis of the case (*a*) representation. The intermediate wave functions, in terms now of those in pure case (*b*), that are derived from the diagonalization of (42) are

$$\psi_{\text{Int. I, II}}=\left(\frac{\pm X+2(J+\frac{1}{2})-\lambda/(J+\frac{1}{2})}{\pm 2X}\right)^{\frac{1}{2}}\psi(N=J-\tfrac{1}{2})$$
$$\pm\left(\frac{\mp X+2(J+\frac{1}{2})-\lambda/(J+\frac{1}{2})}{\mp 2X}\right)^{\frac{1}{2}}\psi(N=J+\tfrac{1}{2}). \tag{43}$$

The upper signs apply to the states $N=J-\frac{1}{2}$ in pure case (*b*), and to the $^2\Pi_{\frac{3}{2}}$ and $^2\Pi_{\frac{1}{2}}$ state in case (*a*) for λ positive and negative respectively. The lower signs apply to states that connect with $N=J+\frac{1}{2}$ in case (*b*), and to $^2\Pi_{\frac{1}{2}}$ and $^2\Pi_{\frac{3}{2}}$ states in case (*a*) for positive and negative values of λ respectively.

In the pure state $N=J-\frac{1}{2}$, $f=N(N+1)=J^2-\frac{1}{4}$ and in state $N=J+\frac{1}{2}$, $f=N(N+1)=(J+1)^2-\frac{1}{4}$. Since this correction term for B has the form N^2 and no matrix elements of the type $\Delta N=\pm1$, for intermediate coupling

$$f_{\text{Int.}}=a^2J^2+(1-a^2)(J+1)^2-\tfrac{1}{4}.$$

Here a and $(1-a^2)^{\frac{1}{2}}$ are the amplitudes of the pure case (*b*) states in the intermediate wave function as given by (43). This becomes, if the constant term is neglected.

$$f_{\text{Int. I, II}}=J^2+\left(\frac{\mp X+2(J+\frac{1}{2})-\lambda/(J+\frac{1}{2})}{\mp X}\right)(J+\tfrac{1}{2}),$$
$$B=B_0\left(1-\frac{D_0}{B_0}f_{\text{Int.}}\right). \tag{44}$$

The states to which the upper or lower signs apply are as explained for (43). Expression (44) reduces to the appropriate forms $N(N+1)+$cnost for both members of the spin doublet in case (*b*) and to $J(J+1)+$const for $^2\Pi_{\frac{1}{2}}$ and $^2\Pi_{\frac{3}{2}}$ states in case (*a*).

In all formulas where B appears, including λ and $\langle\Pi|BL_y|\Sigma\rangle$, it will be corrected according to (44).

5. INTERPRETATION OF EXPERIMENTAL RESULTS—COMPARISON WITH THEORY

(a) Λ-Type Doubling Variation of the Matrix $\langle\Pi|L_y|\Sigma\rangle$ with Rotation

One obtains the separations of the two Λ-type doublet levels (ν_Λ) by subtracting the hyperfine structure (using

[25] E. Hill and J. H. Van Vleck, Phys. Rev. **32**, 250 (1928).

TABLE II. Comparison of experimental and calculated values of the Λ-type doubling separations (ν_Λ) in OH and OD. The experimental values are obtained by subtracting the hyperfine structure from the data of Table I. Calculation A shows a fit with the theory that inciudes terms in both first and second order in $[(E_{\text{rot}} \text{ or } E_{\text{fs}})/E_{\text{el}}]$. In calculation B, in addition, a small variation of $|\langle\Pi|L_y|\Sigma\rangle|^2$ ($\sim$ one part in 1400) from one rotational state to the next is allowed. Centrifugal distortion has been taken into account in A and B (see text).

Molecule	Electronic state	N	J	ν_Λ experimental (Mc/sec)	A ν_Λ(cal.) $-\nu_\Lambda$(exp.)	B ν_Λ(cal.) ν_Λ(exp.)
$O^{16}H$	$^2\Pi_{\frac{1}{2}}$	2	3/2	7 797.59±0.15	−1.29	+1.35
		3	5/2	8 166.08±0.15	+3.86	−2.81
	$^2\Pi_{\frac{3}{2}}$	3	7/2	13 438.41±0.05	−15.14	−6.65
		4	9/2	23 822.98±0.05	−11.19	−6.54
		5	11/2	36 989.41±0.15	+33.11	+11.40
$O^{18}H$	$^2\Pi_{\frac{3}{2}}$	4	9/2	23 474.8 ±0.5	−13.8	−9.7
$O^{16}D$	$^2\Pi_{\frac{1}{2}}$	3	5/2	8 120.37±0.15	−7.56	+2.46
		4	7/2	9 587.93±0.15	−7.64	−1.49
		5	9/2	10 200.71±0.10	−0.25	−3.02
		6	11/2	9 922.78±0.10	+12.39	−4.17
	$^2\Pi_{\frac{3}{2}}$	5	11/2	8 672.36±0.10	−11.60	−1.62
		6	13/2	12 918.01±0.10	−11.16	−1.59
		7	15/2	18 009.60±0.10	−2.24	+1.54
		8	17/2	23 907.12±0.10	+24.29	+12.79

the Interval Rule) from the measured frequencies listed in Table I.

These undisplaced frequencies are compared with the theory that includes both first and second order terms in expansion parameters as given by (22) and (23) above. Centrifugal distortion is taken into account according to (44) which is applied to B, λ and $\langle\Pi|BL_y|\Sigma\rangle$. Of the seven molecular constants (λ, α_p, β_p, B_p, B_s, D_0, $E\equiv E_\Sigma - E_\Pi$) that enter the theoretical expressions the ones that appear in the main term $[\nu_\Lambda^{(1)}]$, aside from D_0, are λ, α_p, and β_p. These three constants will be determined from the present data. The others, including D_0, appear only in the second order term $\nu_\Lambda^{(2)}$ or in the small centrifugal correction to $\nu_\Lambda^{(1)}$ and are known from earlier work[3,18] to an accuracy sufficient for present purposes. The values which were used are listed in Appendix I.

There are hence three parameters to be evaluated from the data for each molecule. For OH these three must satisfy five equations, and the three constants for OD must fit eight equations. One such fit that can be considered as best is compared with the experimental results in Table II (Column A). The values of the constants are, in OH: $\lambda=-7.410$, $\alpha_p=-2358.95$ Mc/sec, $\beta_p=572.99$ Mc/sec; and in OD: $\lambda=-13.890$, $\alpha_p=-1545.99$ Mc/sec, $\beta_p=160.72$ Mc/sec. The deviations appear as systematic functions of J. The average deviation is about 13 Mc/sec in OH and 9.6 Mc/sec in OD or about one part in 2000. One can fit the experimental data with an average deviation of about 15 Mc/sec even when terms in second order ($\nu_\Lambda^{(2)}$) are neglected. Such fits, however, and the constants thereby determined, do not have much meaning since the term $\nu_\Lambda^{(2)}$ is as large as 120 Mc/sec.

For the above calculation (results in Table II, Column A) the matrix $\langle\Pi|L_y|\Sigma\rangle$ involved in the constants α_p, β_p is assumed to be independent of J. We may allow for some variation in the electronic wave function with the change of internuclear distance that results from centrifugal stretching. The order of magnitude of such a variation can be established from the following consideration. A change of the internuclear distance by 100%, for example, would produce a change roughly of the same order in the molecular wave function (and the Λ-type doubling). Hence for infinitesimal displacements

$$\Delta\psi/\psi\sim\Delta r/r=-D_0N(N+1)/2B,$$

where D_0 is the centrifugal distortion constant. We write then approximately

$$(|\langle\Pi|L_y|\Sigma\rangle|^2)_N=(|\langle\Pi|L_y|\Sigma\rangle|^2)_0[1-CN(N+1)], \quad (45)$$

where C is of order D_0/B_0, and one may use the intermediate coupling formula (44) instead of $N(N+1)$.

Introducing this variation in the parameters α_p and β_p and using again (22), (23), and (44) we obtain the fit shown in Column B of Table II. The agreement between calculated and experimental values is considerably better here than above when no variation in the wave function was allowed. The average deviation is reduced to 5.8 Mc/sec in OH and 3.6 Mc/sec in OD or about one part in 3500. The better agreement with theory, in all cases, of the OD data is not surprising in view of the faster convergence of the energy expansion (6) in this molecule $[B(\text{OD})/E\sim\frac{1}{2}B(\text{OH})/E]$. The value of the parameters obtained from this calculation, which we take as the values of the molecular constants are for OH as follows:

$$\lambda^0=-7.444\pm0.017,$$
$$\alpha_p{}^0=-2361.37\pm2.95 \text{ Mc/sec},$$
$$\beta_p{}^0=576.18\pm1.64 \text{ Mc/sec},$$
$$C \text{ in } (45)=(1.2\pm0.5)D_0/B_0;$$

and for OD:

$$\lambda^0 = -13.954 \pm 0.032,$$
$$\alpha_p{}^0 = -1548.99 \pm 2.10 \text{ Mc/sec},$$
$$\beta_p{}^0 = 161.94 \pm 0.61 \text{ Mc/sec},$$
$$C = (1.2 \pm 0.5) D_0/B_0.$$

The superscript 0 indicates that these values apply to the lowest vibrational and rotational levels. For higher rotational states the parameters are to be evaluated from the values given above and (44), (45). With the above value for C, expression (45) represents a variation of about one part in 1400 in the electronic wave function from one rotational state to the next.

The uncertainties quoted in the molecular constants are mostly due to neglected effects in the theory rather than the experimental error. These are

(*a*) The interaction $\gamma \mathbf{N}\cdot\mathbf{S}$, where γ is of order $(m/M)A$. The Λ-type doubling will be affected to the extent that this interaction will influence the intermediate coupling as discussed above. The order of magnitude of the effect is $(m/M)\nu_\Lambda{}^{(1)}$ or about 2.5 Mc/sec for the $J=13/2$ state of $O^{16}D$. Inclusion of this effect would bring the calculated frequencies in somewhat better agreement with the experimental results.

(*b*) The effect of the $^2\Sigma$ state in third order in expansion parameters, contributing terms of the form

$$\left(\frac{A \text{ or } BJ}{E_\Sigma - E_\Pi}\right)^2 \nu_\Lambda{}^{(1)}.$$

This would be about 0.3 Mc/sec for $J=13/2$ in $O^{16}D$.

(*c*) The influence of the $^2\Delta$ state. The Λ-type doubling in the $^2\Delta$ state is[16]

$$\frac{48B^4(J-1)J(J+1)(J+2)}{(E_\Sigma - E_\Pi)^2(E_\Sigma - E_\Delta)}.$$

The corresponding terms in $^2\Pi$ states would be of order

$$\left(\frac{A \text{ or } BJ}{E_\Sigma - E_\Pi}\right)\left(\frac{BJ}{E_\Sigma - E_\Delta}\right)\nu_\Lambda{}^{(1)}.$$

The value of $E_\Sigma - E_\Delta$ is not known. If one assumes it to be comparable to $E_\Sigma - E_\Pi$, this contribution would be of the same magnitude as the one due to the $^2\Sigma$ state in third order [(*b*) above].

(*d*) Centrifugal distortion to order $(B/\omega_{vib})^4$. The rotational constant B has been corrected to order $(B/\omega_{vib})^2$ by (44). The next correction term in the rotational energy has the form $HJ^3(J+1)^3$, where

$$H = \frac{2B^3}{3\omega_{vib}{}^4}(2B^2 - \alpha_e\omega_{vib}).$$

The effect on the Λ-type doubling is

$$\frac{2H}{B}J^2(J+1)^2\nu_\Lambda{}^{(1)},$$

or about 0.1 Mc/sec in $J=13/2$ of $O^{16}D$.

TABLE III. Effects that contribute to or affect the Λ-type doubling. The numerical values apply to the $J=13/2$ state in the $^2\Pi_{\frac{1}{2}}$ level of $O^{16}D$. By taking into account (1)–(4) and using the experimentally determined constants one calculates a frequency $\nu_\Lambda = 12\,916.42$ Mc/sec. The observed value is 1.59 ± 0.10 Mc/sec higher. One sees that the estimated contribution from the neglected effects (5), (6), (7), and (8) is comparable to 1.59 Mc/sec.

Description	Order of magnitude	Numerical value (Mc/sec)
(1) Effect of $^2\Sigma$ state to first order in expansion parameters	$\left(\frac{A \text{ or } BJ}{E_\Sigma - E_\Pi}\right) BJ \equiv \nu_\Lambda{}^{(1)}$	12 957.00
(2) Centrifugal distortion on B to order $(B/\omega)^2$	$\frac{8B^2J^2}{\omega_{vib}{}^2}\nu_\Lambda{}^{(1)}$	−71.49
(3) Effects of $^2\Sigma$ state state to second order	$\left(\frac{A \text{ or } BJ}{E_\Sigma - E_\Pi}\right)\nu_\Lambda{}^{(1)}$	+66.73
(4) Variation of electronic wave function with rotation	$\frac{4B^2J^2}{\omega_{vib}{}^2}\nu_\Lambda{}^{(1)}$	−35.82
(5) Effect of the interaction $\gamma\mathbf{N}\cdot\mathbf{S}$	$\frac{m}{M}\nu_\Lambda{}^{(1)}$	∼2.5
(6) Effect of $^2\Sigma$ state to third order	$\left(\frac{A \text{ or } BJ}{E_\Sigma - E_\Pi}\right)^2 \nu_\Lambda{}^{(1)}$	∼0.3
(7) Effect of $^2\Delta$ state	$\left(\frac{A \text{ or } BJ}{E_\Sigma - E_\Pi}\right)\left(\frac{BJ}{E_\Sigma - E_\Delta}\right)\nu_\Lambda{}^{(1)}$	∼0.3
(8) Centrifugal distortion on B to order $(B/\omega)^3$	$\frac{4B^2J^4}{3\omega_{vib}{}^3}\left(\frac{12B^2}{\omega_{vib}} - \alpha_e\right)\nu_\Lambda{}^{(1)}$	∼0.1

The numerical estimates of the contributions (*a*), (*b*), (*c*) and (*d*), based on the above approximate expressions, are comparable with the deviations between calculated and experimental frequencies (see Table II). We note also that the deviations are seen from Table II to be monotonic functions of J, which is the behavior to be expected from the higher order terms. One may then ascribe the discrepancies (about one part in 3500) to the neglected effects (*a*), (*b*), (*c*), and (*d*). A small part of the deviations may also be due to use of the pure precession hypothesis in calculating centrifugal effects on B. From what follows, the hypothesis would appear to be somewhat inadequate for evaluating the centrifugal effects with accuracy commensurate to that of the data. The various contributions to the Λ-type doubling, with numerical values for a particular value of J, are summarized in Table III.

We compare the present values for the molecular constants in $O^{16}H$ with those previously obtained from ultraviolet work. Our value for λ (-7.444 ± 0.017) is 1.3% lower than the previous value of Dicke and Crosswhite, who reported[3] −7.547. Inspection of their data indicates that the uncertainty may be as large as

TABLE IV. Parameters that describe the Λ-type doubling and values calculated from the pure precession hypothesis. α_p and β_p are in Mc/sec.

Parameter	$O^{16}H$ Experimental	$O^{16}H$ Calculated	$O^{16}D$ Experimental	$O^{16}D$ Calculated
$\lambda(\equiv A/B)$	-7.444 ± 0.017		-13.954 ± 0.032	
α_p	-2361.37 ± 2.95	-3491	-1548.99 ± 2.10	-2172
β_p	576.18 ± 1.64	629	161.94 ± 0.61	179
$\left(\frac{\alpha_p-2\beta_p}{\beta_p}\right)$	-6.098 ± 0.013	$-7.444(=\lambda)$	-11.558 ± 0.025	$-13.954(=\lambda)$

0.8% which may be increased to one percent if one considers uncertainties due to centrifugal distortion, not taken into account in the earlier work. Consideration of the centrifugal effects on λ would actually bring the earlier value somewhat closer to the present one. In that case the two experimental values would be in marginal agreement. We note that the present value of λ is also favored by the magnetic hyperfine results in that the hfs constants determined from the $^2\Pi_{\frac{3}{2}}$ data are more consistent with those in the $^2\Pi_{\frac{3}{2}}$ state if one uses it rather than the earlier value in (33). Only crude values exist in previous literature[3,26] for the specific Λ-doubling constants α_p and β_p. They are -2.3×10^3 Mc/sec and 5.7×10^2 Mc/sec respectively and are in good agreement with the present values -2361.37 ± 2.94 and 576.18 ± 1.65 in $O^{16}H$. The Λ-type doubling in OD is also of the magnitude indicated by ultraviolet work.[27]

It is of interest to compare the experimentally determined constants in the different isotopic species. The constant $(\alpha_p-2\beta_p)$ is directly proportional to B whereas β_p is proportional to B^2. The constant B is not known in $O^{18}H$ but, if one assumes a structure identical with that of $O^{16}H$, the constants $(\alpha_p-2\beta_p)$ and β_p can be derived from those of $O^{16}H$ and the reduced molecular masses. The $O^{18}H$ frequency in Table II has been calculated in this way and agrees very well with the experimental value. One sees that this line is predicted from the theory and the $O^{16}H$ data with an accuracy comparable to that for the $O^{16}H$ lines themselves. The agreement, to one part in 8000, depends on the close similarity of the electronic structure in the two isotopic species.

The experimental value for the ratio

$$[(\alpha_p-2\beta_p)_{OH}/\alpha_p-2\beta_p)_{OD}]$$

is 1.8761 ± 0.0030 compared with 1.8763 for the ratio $(B)_{OH}/(B)_{OD}$. And $(\beta_p)_{OH}/(\beta_p)_{OD})=3.5585\pm0.0035$ compared to 3.5204 for the ratio $[(B)_{OH}/(B)_{OD}]^2$. The agreement is quite good in view of the fact that the constants α_p and β_p depend explicitly on the electronic wave function (through $\langle\Pi|L_y|\Sigma\rangle$) in addition to B. The electron wave function is assumed in this comparison to be identical in OH and OD, and $E_\Sigma-E_\Pi$ in OD is taken to be identical with that in OH (32682.5 cm^{-1}). The result above indicates that a value reported[26,18] for $E_\Sigma-E_\Pi$ in OD, about 10 percent different from that in OH, must be in error. It is also implicitly assumed in the above comparison that the inverse moment of inertia B can be taken as a constant multiplying the matrix $\langle\Pi|L_y|\Sigma\rangle$ in α_p and β_p. This is part of the pure precession hypothesis.[16]

The pure precession hypothesis makes the assumption that the orbital electronic angular momentum is of constant magnitude and precesses at a constant rate about the internuclear axis. Under these conditions the constant α_p becomes

$$\frac{4(A+2B)|\langle\Pi|L_y|\Sigma\rangle|^2}{E_\Sigma-E_\Pi}=\frac{(2A+4B)B}{E_\Sigma-E_\Pi},$$

and

$$\beta_p=\frac{2B^2}{E_\Sigma-E_\Pi}.$$

The values of the constants so obtained are compared in Table IV with the experimental results. One sees that the agreement is only to within 35%. Despite this, the pure precession hypothesis is quite useful since one can estimate from it the magnitude of these higher order effects in the absence of precise experimental work.

(b) Relative Line Intensities

The observed relative line intensities confirm the prediction of the intermediate coupling formula (39) as to the behavior of the electric dipole matrix element in the transition from Hund's case (*a*) to (*b*). The observed intensities in the $^2\Pi_{\frac{3}{2}}$ lines relative to those in $^2\Pi_{\frac{1}{2}}$ state are larger than one would predict from Hund's case (*a*) quantization [or smaller than predicted from case (*b*)] and appear to vary from one rotational state to next in accordance with (39).

(c) Magnetic Hyperfine Structure and Coupling Constants

The magnetic hyperfine structure results are fitted with (33) above. The hyperfine doubling term in d is a measure of the difference in the hyperfine structures of the two Λ-doublet levels, which equals the frequency difference of the two main ($\Delta F=0$) lines in OH or the

[26] R. S. Mulliken and A. Christy, Phys. Rev. **35**, 87 (1931).
[27] M. Ishaq, Proc. Roy. Soc. (London) **159**, 110 (1937); additional references are given in reference 18.

difference between the two extreme members of the main hyperfine triplet in OD (see Fig. 2). Denoting this frequency difference by $\Delta\nu_1$, we have from (33), in OH:

$$\Delta\nu_1=d\left(\frac{\pm X-2+\lambda}{\pm 2X}\right)\frac{(J+\frac{1}{2})^2}{J(J+1)}, \tag{46}$$

and in OD:

$$\Delta\nu_1=d\left(\frac{\pm X-2+\lambda}{\pm 2X}\right)\frac{2(J+\frac{1}{2})^2}{J(J+1)}, \tag{47}$$

where the upper and lower signs apply to the $^2\Pi_{\frac{3}{2}}$ and $^2\Pi_{\frac{1}{2}}$ states respectively. The hyperfine results (Table I) for the main lines are fitted with the single parameters d in each of the two isotopic species. The values obtained are, in Mc/sec,

$$d(\mathrm{OH})=57.0\pm1.5 \quad \text{and} \quad d(\mathrm{OD})=8.69\pm0.16.$$

The calculated and experimental values of $\Delta\nu_1$, are compared in Table V. The agreement is to about 2% and quite satisfactory in view of the approximations used in deriving (33).

The hyperfine structure in $O^{18}H$ should according to theory be equal, within the present experimental error, to that in $O^{16}H$. Our measured value for $\Delta\nu_1$ in $O^{18}H$ for $J=9/2$ is 9.6 ± 0.5 Mc/sec compared to 8.72 ± 0.10 in $O^{16}H$. The indicated discrepancy is so marginal that more precise measurements are required to establish any real difference in the hfs of the two species. Such a difference would be rather surprising.

The other experimental information, besides the hyperfine doubling, is the frequency separation of the two satellite lines ($\Delta F=\pm1$). This frequency separation is equal to the sum of the hyperfine structures in the two Λ-doublet levels (see Fig. 2). From (33) we have, in OH

$$\Delta\nu_s\equiv\Delta(\nu_{F=J+\frac{1}{2}}-\nu_{F=J-\frac{1}{2}})$$
$$=\frac{2J+1}{\pm4J(J+1)X}\left[2a(\pm2X+2-\lambda)\right.$$
$$\left.+4b(J-\tfrac{1}{2})(J+\tfrac{3}{2})+(b+c)(\pm X+4-2\lambda)\right], \tag{48}$$

where the upper and lower signs in front of X apply to the $^2\Pi_{\frac{3}{2}}$ and $^2\Pi_{\frac{1}{2}}$ states respectively. Because of their low intensity, we have been able to observe these satellites only in the strong $J=9/2$ spectrum of $O^{16}H$ in the $^2\Pi_{\frac{3}{2}}$ state. In this state $\Delta\nu_s=31.3\pm0.8$ Mc/sec. From this information alone the three constants a, b, and c involved in (48) cannot be determined. If one assumes that the electron with the orbital angular momentum is also the one that carries the free spin, then the relation $c=3(a-d)$ holds and one is left in (48) with the two constants a and b. In a pure p state $\psi^2(0)=0$ and the constant b is from (31) simply $-c/3$. However, a small admixture of s state (about 2.5%) has been found in the similar cases of the $O^{16}O^{17}$ and NO molecules[21,28] to contribute to the hyperfine structure an amount comparable to the classical dipole-dipole part of the interaction. Calculations based on atomic orbital approximations and on the NO results[20] indicate that only a crude value of a (accurate to about 40 percent) can be obtained if one assumes $\psi^2(0)=0$ and solves (48) for a using the experimental result for $\Delta\nu_s$. The value so derived is

$$a=58\pm20 \text{ Mc/sec},$$

where the correct value is probably closer to the lower rather than the upper limit. Measurements of these satellites are needed in additional rotational states to determine the constants b and c and reduce the uncertainty in a. This would require a spectrometer of somewhat higher sensitivity.

Expression (33) predicts that the satellites must be symmetrically spaced with respect to the main lines. The observed satellite frequencies in the $^2\Pi_{\frac{3}{2}}$ state (Table I) are, within experimental error, in agreement with this requirement. It is interesting to note that the theory, with the values for the constants given above, indicates that in the $^2\Pi_{\frac{1}{2}}$ state the satellites should be inside the main lines rather than outside as observed in $^2\Pi_{\frac{3}{2}}$ state. This is due to the preponderance of the hyperfine doubling term over the rest of the hyperfine structure in the $^2\Pi_{\frac{1}{2}}$ state, which inverts the hyperfine components in the lower Λ-doublet level. Such behavior has been observed in the spectrum of NO.[29,30]

TABLE V. Magnetic hyperfine structure in OH and OD. $\Delta\nu_1$ designates the frequency difference between the two main ($\Delta F=0$) lines in OH or the difference between the two extreme members of the main hyperfine triplet in OD. $\Delta\nu_s$ denotes the frequency separation between the two satellite ($\Delta F=\pm1$) lines in OH (see Fig. 2). All values are in Mc/sec.

Molecule	Electronic state	N	J	$\Delta\nu_1$ exp.	$\Delta\nu_1$ calc.
$O^{16}H$	$^2\Pi_{\frac{1}{2}}$	2	3/2	59.56 ± 0.25	58.94
		3	5/2	53.43 ± 0.25	54.47
	$^2\Pi_{\frac{3}{2}}$	3	7/2	6.74 ± 0.10	6.56
		4	9/2	8.72 ± 0.10	8.79
		5	11/2	10.96 ± 0.30	10.77
$O^{18}H$	$^2\Pi_{\frac{3}{2}}$	4	9/2	9.6 ± 0.5	8.74
$O^{16}D$	$^2\Pi_{\frac{1}{2}}$	3	5/2	17.44 ± 0.25	17.36
		4	7/2	16.75 ± 0.25	16.77
		5	9/2	16.50 ± 0.20	16.25
		6	11/2	15.49 ± 0.20	15.78
	$^2\Pi_{\frac{3}{2}}$	5	11/2	<2.1	1.70
		6	13/2	<3.0	2.14
		7	15/2	<3.0	2.53
		8	17/2	<3.0	2.90
	Also				
$O^{16}H$	$^2\Pi_{\frac{3}{2}}$	4	9/2	$\Delta\nu_s=31.3\pm0.8$	$\Delta\nu_s=31.31$

[28] Miller, Townes, and Kotani, Phys. Rev. **90**, 452 (1953).
[29] C. A. Burrus and W. Gordy, Phys. Rev. **92**, 1437 (1953).
[30] Gallagher, Bedard, and Johnson, Phys. Rev. **93**, 729 (1954).

(d) Molecular Electronic Structure

Parameters that depend on the electronic wave functions are involved in the present results on the Λ-type doubling and the hyperfine structure and can be used as tests of proposed schemes for the electronic structure of the molecule.

The most important structure for OH is expected to be[26]

$$(1s\sigma)^2(2s\sigma)^2(2p\sigma)^2(2p\pi)^3.$$

In Λ doubling, the experimentally determined parameters α_p and β_p depend on the electronic wave function through the quantity $|\langle\Pi|L_y|\Sigma\rangle|^2$. The above structure for OH with the pure precession hypothesis gives values for the Λ-type doubling which agree, at least qualitatively, with the experimental results (Sec. 5a above).

More definite information on the distribution of the unpaired electron orbital and spin angular momenta in the molecule is provided by the hyperfine structure parameters a and d. From the experimetal values of these quantities and using the definitions (31), one derives, in OH:

$$(1/r^3)_{Av}=(0.75\pm0.25)\times10^{24}\ \text{cm}^{-3},$$
$$(\sin^2\chi/r^3)_{Av}=(0.490\pm0.013)\times10^{24}\ \text{cm}^{-3}.$$

For OD,

$$(\sin^2\chi/r^3)_{Av}=(0.486\pm0.009)\times10^{24}\ \text{cm}^{-3},$$

in excellent agreement with the value for OH. The uncertainty in the value of $(1/r^3)_{Av}$ is due to the assumption that $\psi^2(0)=0$. As already mentioned, the correct value may be closer to the lower limit than to the upper limit.

Similar experimental results in the $O^{16}O^{17}$ and NO molecules have been used in studying the electronic structure.[21,28,31] In these cases one finds the appropriate combination of atomic wave functions (which is taken as the electronic structure) that yields the observed values of the hyperfine parameters. Effects of overlapping can be neglected since for atoms like N and O the parts of the electron distribution which contribute substantially to the hyperfine interaction are, by comparison with the internuclear distance, quite close to the nuclei.

In OH the observed constants are of the order of magnitude one would expect from such a scheme. One cannot, however, use a similar simple analysis to determine the electronic structure since in this case the oxygen nucleus is well within the $2p$ electron orbit of the hydrogen and a $2p$ atomic orbital would hence be a very poor approximation. The experimental results, given also in Table VI, can be used as definite tests of molecular wave functions that may be constructed, but rather careful calculations must be made to evaluate the expected hyperfine structure from the chosen wave functions.

[31] Townes, Dousmanis, White, and Schwarz, Trans. Faraday Soc. (to be published).

TABLE VI. Parameters, derived from the magnetic hyperfine structure data, that describe the unpaired electron distribution in OH and OD. The vector **r** is the radius vector from the proton or deuteron to the unpaired electron and χ the angle between **r** and the internuclear axis. These values are in units of 10^{24} cm^{-3}.

Parameter	Experimental value $O^{16}H$	$O^{16}D$
$(1/r^3)_{Av}$	0.75±0.25	
$(\sin^2\chi/r^3)_{Av}$	0.490±0.013	0.486±0.009

The present results yield information on the unpaired electron distribution about the proton or deuteron. Experimental results on $O^{17}H$ would be interesting since they would involve the hyperfine interaction of O^{17} and hence would measure the electron distribution about the oxygen. For O^{17}, simple calculations could give approximate values of the hyperfine constants to be expected from a given electronic structure.

6. LINE INTENSITIES AND RADICAL ABUNDANCE—SURFACE TESTS AND THE LIFE TIME OF OH IN GLASS

The strongest of the observed OH spectra is that due to the $J=9/2$ state in the $\Pi_{\frac{3}{2}}$ level. Under the best conditions these lines were detected by the spectrometer with a signal to noise ratio of approximately 1000:1. The signal to noise ratio was about 10:1 for the $J=11/2$ spectrum of $O^{16}D$ in the $\Pi_{\frac{3}{2}}$ state, which is the weakest of the observed Λ-type doubling transitions. From these values, using the figure of 0.5×10^{-8} cm^{-1} for the minimum detectable absorption with this instrument, one sees that the intensity of the observed lines of OH and OD ranges approximately from 5×10^{-6} cm^{-1} to 5×10^{-8} cm^{-1}. From the line intensity, combined with the line breadth (~1 Mc/sec) one may derive an approximate value for the radical abundance in the absorption cell. The following conditions however must be noted:

(1) It is necessary to assume that the radicals are in thermal equilibrium with the walls. This assumption is on rather safe ground since a radical makes approximately 10^5 collisions between the time it leaves the discharge tube and enters the absorption cell.

(2) One has to assume a reasonable line breadth at the operating total pressures.

(3) The electric dipole moment of the molecule is not well known. We have used the tentative value[10] of 1.5 Debye units.

The value obtained for the maximum percentage of radicals present in the gas is between 3% and 30%. The large uncertainty quoted comes from estimates of the errors which may be produced by the uncertainties listed above. A previous spectroscopic measurement of OH radical abundance in the products of a water discharge is available.[12] In this method the intensities of ultraviolet absorption due to OH produced by thermally dissociated water and by discharge were

compared. A partial pressure of OH of approximately 1×10^{-3} mm Hg was found at a total pressure near 1 mm Hg. The present work indicates the presence of very much higher radical concentrations.

Since different conditions were used in the two measurements, the two values are not necessarily inconsistent. In the earlier work a pulsed dc discharge was used with a total current of 180 ma and a current density of 9.5 ma/cm^2. In the present apparatus measurements on a dc discharge indicate that at 0.1 mm Hg optimum intensity is produced with a total current of 400 ma and a density of 80 ma/cm^2. Maximum line intensity is produced by higher discharge currents as the pressure is increased and one would expect that higher currents are needed at 1 mm Hg. In addition, the radical abundance may be expected to be lowered by the use of a pulsed discharge.

No quantitative explanation of the variation of the line intensity with discharge current and pressure will be attempted here. In the present experiments the effects of changing radical production and of varying recombination are not easily separated. It seems qualitatively that at different pressures the discharge conditions producing a relative maximum in line intensity all correspond to approximately the same average electron energies in the discharge tube. That the absolute maximum occurs at the high-pressure end of the available range suggests that wall rather than volume recombination is the dominant effect in removing the radicals.

In order to determine the effect of recombination on destroying the radicals during their transit through the absorption cell, measurements of radical abundance at different points in the cell were made. By passing the modulating current through only a portion of the solenoid one may detect absorption due to radicals in the corresponding part of the cell. Measurements were made by applying the modulation to two 10 cm lengths of the coil one at each end of the cell, which in this case was 75 cm long. The measured intensity difference was approximately 10%. The actual difference in radical abundance at the two ends is somewhat greater because of the finite length of the test intervals including the effect of fringing fields. From this figure we infer that the radical lifetime is approximately equal to the time required by a molecule to traverse the cell. This figure is approximately $\frac{1}{3}$ sec and is in good agreement with spectroscopic measurements in the ultraviolet region.[2]

In addition to spectroscopic techniques, two other methods for detecting OH and studying its properties have been reported in previous literature. These involve (*a*) measurements of the temperature rise of a probe coated with KCl on which the OH radicals are presumed to recombine,[5] and (*b*) the H_2O_2 concentration measurement[4] described in Sec. 2b above. These tests were used in the earlier part of this work to make sure that OH radicals were in the absorption cell. Once the microwave spectrum was found, however, it became apparent that these tests (at least to the extent that we have been able to reproduce and apply them) give results that are not correlated with the OH concentration as measured by the intensity of the microwave lines. The evidence for this has already been published elsewhere.[7]

Some tests have been made to determine whether the presence of certain surfaces in the path of gas flow would affect the concentration of the OH radicals. The OH concentration would decrease if a particular substance either directly combines with OH or simply provides a convenient surface for radical recombination.

A side tube was blown in the tube connecting the discharge to the absorption cell. In this side tube a glass rod was introduced, bearing on one end the substance to be tested and on the other a magnetic core (glass-covered) so that the rod could be moved from outside with a small magnet. Thus line intensities could be measured with the sample in and out of the path of radical flow, all other conditions being the same. The following surfaces decreased greatly the OH concentration: Copper, graphite, nickel, and kovar. Substances that do not appreciably affect the OH are apiezon wax, Teflon, glyptal, potassium chloride, and aluminum. Mica is found to decrease the OH but not as effectively as members of the first group.

These results, especially the ones that indicate that a substance does not affect the OH, are to be taken with some reservations. These are (*a*) the surface exposed to the discharge products is rather limited in size ($\sim\frac{1}{4}$ cm^2, tube cross section ~1 cm^2); (*b*) the time of exposure also was rather short. We have carried out more elaborate tests with extended aluminum surfaces which indicate that, despite the result of the test described above, the OH does not live long in aluminum environment. Thus if an aluminum tube is substituted for a large (5 inches) section of the glass tube that connects the discharge to the absorption cell the line intensity decreases steadily to zero in a matter of a few minutes. This indicates an alteration of the aluminum oxide surface which increases its ability to destroy OH.

7. CONCLUSION

The experiments on the microwave spectrum of the free OH radical provide detailed information on finer effects in the energy level structure such as the Λ-type doubling and magnetic hyperfine structure. The experimental accuracy for effects of the former kind is for the first time high enough to provide an adequate check on the theory. The results are in agreement with theory to the expected accuracy of the latter. The magnetic hyperfine structure yields parameters that describe the distribution of electronic angular momentum in the molecule and are directly connected to the electronic structure. In addition, the microwave spectrum can be used in determining the lifetime of the radical and in studying its reactivity with various substances. Results

obtained so far give rise to substantial hope that microwave techniques can be quite useful in this direction for other radicals as well as for OH.

8. ACKNOWLEDGMENTS

This work has benefited greatly from the aid of the personnel of the Columbia Radiation Laboratory, to whom we wish to express our appreciation. In particular we wish to acknowledge substantial contributions from Dr. W. A. Hardy and from Dr. A. L. Schawlow, who initiated experimental work on the OH radical.

APPENDIX I. NOTATION

$\mathbf{S}, \mathbf{I}, \mathbf{L}(\mathbf{\Lambda})$	Electron spin, nuclear spin, electronic orbital angular momentum.
$\mathbf{N}$	Angular momentum of molecule exclusive of electron and nuclear spin.
$\mathbf{J}$	Angular momentum exclusive of nuclear spin.
$\mathbf{F}$	Total angular momentum.
Λ, Σ, Ω	Quantum numbers associated with L_z, S_z, J_z.
A	Fine structure interaction constant (energy $=A\mathbf{L}\cdot\mathbf{S}$).
B_p	Rotational constant in $^2\Pi$ state (18.515 cm^{-1} in OH, 9.868 cm^{-1} in OD).
B_s	Rotational constant in $^2\Sigma$ state (16.961 cm^{-1} in OH, 9.03 cm^{-1} in OD).
λ	A/B_p.
X	$[4(J+\frac{1}{2})^2+\lambda(\lambda-4)]^{\frac{1}{2}}$.
D_0	Centrifugal distortion constant (0.00187 cm^{-1} in OH, 0.00052 cm^{-1} in OD).
E	$E_\Sigma^{\cdot}-E_\Pi$ (32 682.5 cm^{-1} in OH, we use the same value in OD).
α_p	$4\sum_{\Sigma\text{-states}}(-1)^s\dfrac{\langle\Pi\vert AL_y+2BL_y\vert\Sigma\rangle\langle\Sigma\vert BL_y\vert\Pi\rangle}{E_\Sigma-E_\Pi}$
β_p	$4\sum_{\Sigma\text{-states}}(-1)^s\vert\langle\Pi\vert BL_y\vert\Sigma\rangle\vert^2/(E_\Sigma-E_\Pi)$.
α_s, β_s	same as α_p, β_p except that the summation is over all Π rather than Σ states.

The values of the constants B, D_0, and E are from references 3, 18. The values of D_0 and E for OD quoted in 18 must be in error (see text). The value for D_0 given above has been calculated from B and ω_{vib}. Presently determined values for λ, α_p, and β_p are given in Table IV.

APPENDIX II. MATRIX ELEMENTS OF H_1 (AFTER VAN VLECK[16])

$$(\Sigma_{\frac{1}{2}}|H_1|\Sigma_{\frac{1}{2}})=(\Sigma_{-\frac{1}{2}}|H_1|\Sigma_{-\frac{1}{2}})=B_s[J(J+1)+\tfrac{1}{4}]+E\equiv E+\alpha'\equiv\alpha,$$

$$(\Pi_{\frac{1}{2}}|H_1|\Pi_{\frac{1}{2}})=(\Pi_{-\frac{1}{2}}|H_1|\Pi_{-\frac{1}{2}})=B_p[J(J+1)+\tfrac{1}{4}]-\tfrac{1}{2}A\equiv\beta,$$

$$(\Pi_{\frac{3}{2}}|H_1|\Pi_{\frac{3}{2}})=(\Pi_{-\frac{3}{2}}|H_1|\Pi_{-\frac{3}{2}})=B_p[J(J+1)-7/4]+\tfrac{1}{2}A\equiv\gamma,$$

$$(\Sigma_{\frac{1}{2}}|H_1|\Sigma_{-\frac{1}{2}})=(\Sigma_{-\frac{1}{2}}|H_1|\Sigma_{\frac{1}{2}})=B_s(J+\tfrac{1}{2})\equiv(-1)^s\delta,$$

$$(\Pi_{\frac{3}{2}}|H_1|\Pi_{\frac{1}{2}})=(\Pi_{-\frac{3}{2}}|H_1|\Pi_{-\frac{1}{2}})=B_p[(J-\tfrac{1}{2})(J+\tfrac{3}{2})]^{\frac{1}{2}}\equiv\epsilon,$$

$$(\Pi_{\frac{1}{2}}|H_1|\Sigma_{-\frac{1}{2}})=(-1)^s(\Pi_{-\frac{1}{2}}|H_1|\Sigma_{\frac{1}{2}})=2\langle\Pi|BL_y|\Sigma\rangle(J+\tfrac{1}{2})\equiv(-1)^s\zeta,$$

$$(\Pi_{\frac{3}{2}}|H_1|\Sigma_{\frac{1}{2}})=(-1)^s(\Pi_{-\frac{3}{2}}|H_1|\Sigma_{-\frac{1}{2}})=2\langle\Pi|BL_y|\Sigma\rangle[(J-\tfrac{1}{2})(J+\tfrac{3}{2})]^{\frac{1}{2}}\equiv\eta,$$

$$(\Pi_{\frac{1}{2}}|H_1|\Sigma_{\frac{1}{2}})=(-1)^s(\Pi_{-\frac{1}{2}}|H_1|\Sigma_{-\frac{1}{2}})=\langle\Pi|AL_y+2BL_y|\Sigma\rangle\equiv\theta.$$

The following phase conventions are observed:

$$\pm i\langle\Sigma|S_x|\Sigma\pm1\rangle=\langle\Sigma|S_y|\Sigma\pm1\rangle=\tfrac{1}{2}[S(S+1)-\Sigma(\Sigma\pm1)]^{\frac{1}{2}},$$

$$\langle\Sigma|S_z|\Sigma\rangle=\Sigma,\quad\langle\Omega|J_z|\Omega\rangle=\Omega,$$

$$\pm i\langle\Omega|J_x|\Omega\pm1\rangle=-\langle\Omega|J_y|\Omega\pm1\rangle=\tfrac{1}{2}[J(J+1)-\Omega(\Omega\pm1)]^{\frac{1}{2}}.$$

Because of the cylindrical symmetry of the molecular field about the internuclear axis (z-direction):

$$\pm i\langle\Lambda|L_x|\Lambda\pm1\rangle=\langle\Lambda|L_y|\Lambda\pm1\rangle.$$